Indian journal of
Engineering

Optimizing Solar Power: Advanced Maximum Power Point Tracking Via Fuzzy Logic for Enhanced Performance and Efficiency

Mujammal Ahmed Hasan Mujammal[1], Ali Nadhim Jbarah Almakki[2], Giulio Lorenzini[3*], Mohammed Abdulelah Albasheri[1], Abdelhafidh Moualdia[1]

To Cite:
Mujammal MAH, Almakki ANJ, Lorenzini G, Albasheri MA, Moualdia A. Optimizing Solar Power: Advanced Maximum Power Point Tracking Via Fuzzy Logic for Enhanced Performance and Efficiency. *Indian Journal of Engineering*, 2025, 22, e10ije1686
doi: https://doi.org/10.54905/disssi.v22i58.e10ije1686

Author Affiliation:
[1]University of Dr Yahia Fares, Department of Electrical Engineering and Automatic Research Laboratory (LREA), Medea, Algeria
[2]University of Diyala, College of Engineering, Iraq
[3]Università di Parma, Department of Industrial Systems and Technologies Engineering, Parma, Italy

[*]**Corresponding Author:**
Dr. Giulio Lorenzini,
Università di Parma, Department of Industrial Systems and Technologies Engineering, Parma, Italy; Email: bkmech@tce.edu

Peer-Review History
Received: 12 April 2024
Reviewed & Revised: 21/May/2024 to 01/June/2025
Accepted: 25 June 2025
Published: 18 July 2025

Peer-Review Model
External peer-review was done through double-blind method.

Indian Journal of Engineering
pISSN 2319–7757; eISSN 2319–7765

DISCOVERY
SCIENTIFIC SOCIETY

ABSTRACT

This research presents an advanced Maximum Power Point Tracking (MPPT) strategy that uses a Fuzzy Logic Controller (FLC) to improve the efficiency and performance of solar power systems. Classic MPPT techniques, such as fractional open-circuit voltage (FOCV), incremental conductance (INC), and perturbation and observation (P&O), often encounter complex structures, slow responses to sudden environmental variations, and inaccurate tracking, leading to significant energy losses and decreased system efficiency. The system utilizes the error and the difference in error (E & ΔE) between the predicted and actual inputs as inputs, and generates the duty cycle (D) as the output. By the circumstances of broad range of climatic conditions, the experiments and simulations involving irradiance levels ranging from 750 W/m² to 1000 W/m² and temperatures varying from 20°C to 45°C, prove the efficacy of the proposed FLC algorithm. These tests demonstrate the system's adaptability to environmental changes. Quantitative results demonstrate a substantial efficiency enhancement of 0.83% over conventional perturbation and observation (P&O) methods, which achieve 0.65%. The result demonstrates that not only is the FLC-based MPPT strategy effective and robust, but it is also well-suited in practice, providing a scalable and effective solution for maximizing solar energy exploitation.

Keywords: Fuzzy Logic, Solar Power, Computational Complexity, Renewable Energy, Adaptive Control.

1. INTRODUCTION

PV systems have become a more attractive renewable energy option in both commercial and academic settings in recent years. This is particularly due to the challenges associated with conventional fossil fuel energy sources. The existence of oil production monopolies in some countries, disputes over oil resources, ecological pollution, and the increasing annual energy consumption rate have emphasized the need for alternative energy sources. Solar energy is a prominent kind of sustainable energy due to its capacity as a reliable and eco-friendly power supply (Mujammal et al., 2024a).

To improve and increase the efficiency of photovoltaic (PV) systems under varying conditions (irradiation and temperature), several methods can be employed, such as MPPT techniques and enhancing PV materials. However, the development of efficient (MPPT) algorithms still represents the least costly option (Albasheri et al., 2024). The performance of PV systems can be significantly improved by implementing an efficient MPP tracking method and optimum tuning of the DC/DC converter (Rabaia et al., 2021). In the current research work, a solar system controlled with the traditional (P&O) method was designed and implemented, which provided an output power of 200 watts from the (PV) panels. A DC-DC converter is used to increase the power output generated from the (PV) panels (Salman et al., 2018) with a 200-W power output from the (PV) panels. In (Bhan et al., 2021), the buck-boost converter is used along with the P&O algorithm to raise the power of PV system panels.

The constant voltage approach is a supplementary method used in the determination of the (MPP) (Liu 2017). It is employed in order to provide rapid tracking, simple configuration, and flexible implementation but is characterized by high levels of oscillation and high rates of error that undermine the total system accuracy. The incremental conductance method is adequately discussed in the literature (Shang et al., 2020). Although the incremental conductance approach has demonstrated decent convergence tracking (Shang et al., 2020; Albasheri et al., 2025b), the constant step size causes additional oscillations during operation at the maximum power point (MPP). This phenomenon deteriorates the tracking time and reduces the efficiency of solar cells. To eliminate the drawbacks inherent to fixed step sizes, recent developments have encouraged the application of variable step sizes to the incremental conductance approach (Chuang et al., 2020). This method involves the adjustment of the slope of the photovoltaic panel to change the step size as well as requires manual calibration depending on irradiance intensity. These aspects are hindrances in applying this method. A new version has been developed (Owusu-Nyarko et al., 2021) which includes an independent scale factor along with adjustments in the slope angle.

A new variant has recently proposed, as referred to (Ali et al., 2023; Basha and Rani, 2020) includes an independent scale factor in addition to adjustments to the slope angle. In addition, the authors presented a comparative study of various conventional and soft-deciding maximum power point tracking (MPPT) techniques for photovoltaic panels, utilizing high step-up converters to achieve the optimal duty cycle. Moreover, an extensive literature review proposes an MPPT technique based on a predictive control scheme. Although predictive control has demonstrated acceptable performance, its algorithmically complex structure and computationally demanding requirements make it unsuitable to address sudden changes in the environment, i.e., irradiance and temperature turbulences (Omar and Haoyu, 2020; Mujammal et al., 2023).

Simple (MPP) tracking models used in solar power systems are challenged by environmental changes but lack the ability to accurately track the MPP during sudden changes in irradiation and temperature. In addition, the existence of partial shading leads to the presence of several local maxima, thereby making these methods challenging to find the global (MPP). Models designed to solve these challenges often introduce complexity and expense to the system, thereby limiting their applicability to small or low-cost applications. Also, most conventional methods suffer from slow convergence, thereby minimizing overall system efficiency in varying environmental conditions (Benyoucef et al., 2024). Hardware constraints also restrict flexibility, as these methods tend to rely on particular designs, thereby limiting their ability to accommodate other solar system designs.

Recent advances in MPPT methods have brought about novel solutions to the constraints in traditional approaches, following recent advancements in computational and control technologies (Mujammal et al., 2025). Machine learning and AI, including neural networks (NNs) and reinforcement learning, enable real-time and significant adaptive MPPT even under complex scenarios, such as partial shading. Metaheuristic algorithms, such as PSO, GAs, and GWO, are highly effective in finding the global maximum in cases of non-linearity and multi-peak landscapes. Hybrid approaches that integrate traditional methods, such as perturb and observe (P&O) (Mousa et al., 2020; Albasheri et al., 2025a) or IC methods with newar approaches such as Fuzzy logic or metaheuristics, enhance efficiency with simplicity being preserved (Mujammal et al., 2025). Evolve dynamically in response to environmental modifications or predicted conditions for anticipatory tracking. Nature-inspired approaches, such as ant colony optimization and artificial bee colony algorithms, offer higher convergence rates and accuracy. IoT integration enables real-time monitoring and centralized optimization, while sophisticated energy management policies enhance system performance overall by integrating energy storage and grid interaction. All these advancements are aimed at improving the efficiency, flexibility, and reliability of MPPT with different operating conditions.

The rationale behind the choice of the suggested (FLC) in the MPPT method in PV systems is its superior capability in handling nonlinearities, uncertainties, and environmental dynamic circumstances associated with photovoltaic systems. Unlike the conventional MPPT algorithms, FLC does not need a specific mathematical model, which makes it quite robust and effective under dynamic irradiance and temperature. Its expert-knowledge-based rule structure allows implementation with the guarantee of adaptability to rapidly varying conditions without periodic retuning. In addition, FLC reduces steady-state oscillations close to the MPP, thus making the convergence softer and faster, and improving the overall energy harvesting efficiency. It is also noise and sensor-inaccuracy-tolerant, which makes it provide consistent performance regardless of disturbances. The aforementioned varied points of FLC make it not only a theoretically sound choice but also a highly satisfactory and practical key to optimizing the power harvesting capabilities of stand-alone PV systems.

The innovation in the suggested algorithm lies in its adaptive rule-based strategy, which allows accurate and quick tracking of the global MPP in various dynamic scenarios and partial shading. It minimizes steady-state ripples, improves stability, and works efficiently in various configurations without relying on fixed models providing a robust solution for solar PV energy harvesting maximization.

In this research, a new (MPPT) control constructed on a (FLC) algorithm is proposed to enhance the output efficiency of solar power systems. The inspiration of this project is to utilize the various strengths of FLC, such as its superior flexibility and simplicity, its ability to mimic human-like cognitive reasoning, and its superiority in the creation of non-linear functions. Under the guidance of experts, FLC offers assistance in the implementation of flexible constraints and offers an efficient solution to manage uncertain data. The novelty of this work lies in the integration of FLC within the MPPT control, which dynamically adjusts to changing environmental conditions, ensuring rapid convergence to the (MPP) without the need for a precise mathematical model this new approach enhances the speed and accuracy of monitoring along with the strength and reliability of the solar power system. Further, it serves to advance the field by simplifying the control mechanism and reducing implementation costs. (Benyoucef et al., 2024).

The proposed FLC-MPPT algorithm offers significant theoretical benefits, as it effectively addresses prevailing research limitations by overcoming key drawbacks of both conventional and advanced MPPT techniques. It addresses the slow-convergence issue in a commendable manner while further enhancing performance under dynamic environmental conditions. Adaptive FLC investigates the complexity of seeking the global maximum power point under conditions of partial shading. Moreover, the method serves to fill the gap that exists between simplicity and higher effectiveness by offering a computationally efficient option for complicated models such as Particle Swarm Optimization (PSO) (Khare and Rangnekar 2013) or neural network (NN) (Mujammal et al., 2021) (Mujammal et al., 2024) Algorithms that necessitate intensive computing power or large training. The Boost Converter Design section outlines the structural and functional characteristics of the DC/DC boost converter used for efficient energy conversion. The MPPT method Based on FLC presents the proposed fuzzy logic-based MPPT algorithm, outlining its structure, operation, and advantages. The analysis of the proposed algorithm is implemented through simulation results that compare its efficiency across different environments. Then, experimental results are provided that prove the algorithm's practicality and run-time feasibility, as confirmed by implementation on a hardware setup. Finally, a summary of the significant conclusions of the proposed algorithm is provided.

2. METHODOLOGY

This study follows a systematic and step-by-step approach to design, simulate, and experimentally validate a (FLC) for (MPPT) of (PV) systems. The procedure entails simulations in MATLAB/Simulink with real-time implementation using the Dspace platform. The approach includes the following steps in sequence:

Step 1. Design of the MPPT Model Using Fuzzy Logic

The initial phase entails the designing of the MPPT algorithm in terms of fuzzy logic concepts. In the MATLAB/Simulink environment, the controller is programmed such that the fuzzy logic rules, membership functions, and decision logic are established for the maximization of solar panel power output (Albasheri et al., 2025c).

Step 2. Simulation and Analysis

Following the design of the fuzzy logic controller, simulations are run to evaluate its performance at different environmental conditions (e.g., irradiance and temperature changes). The principal objective is to verify the controller's capability to effectively track the MPP.

Step 3. Conversion to Dspace-Compatible File

After obtaining successful simulation results, the control algorithm is translated into a real file that can be used with the Dspace system. This includes interfacing the algorithm with Analog-to-Digital Converters (ADCs) for measurements as inputs and Digital-to-Analog Converters (DACs) for commands as outputs.

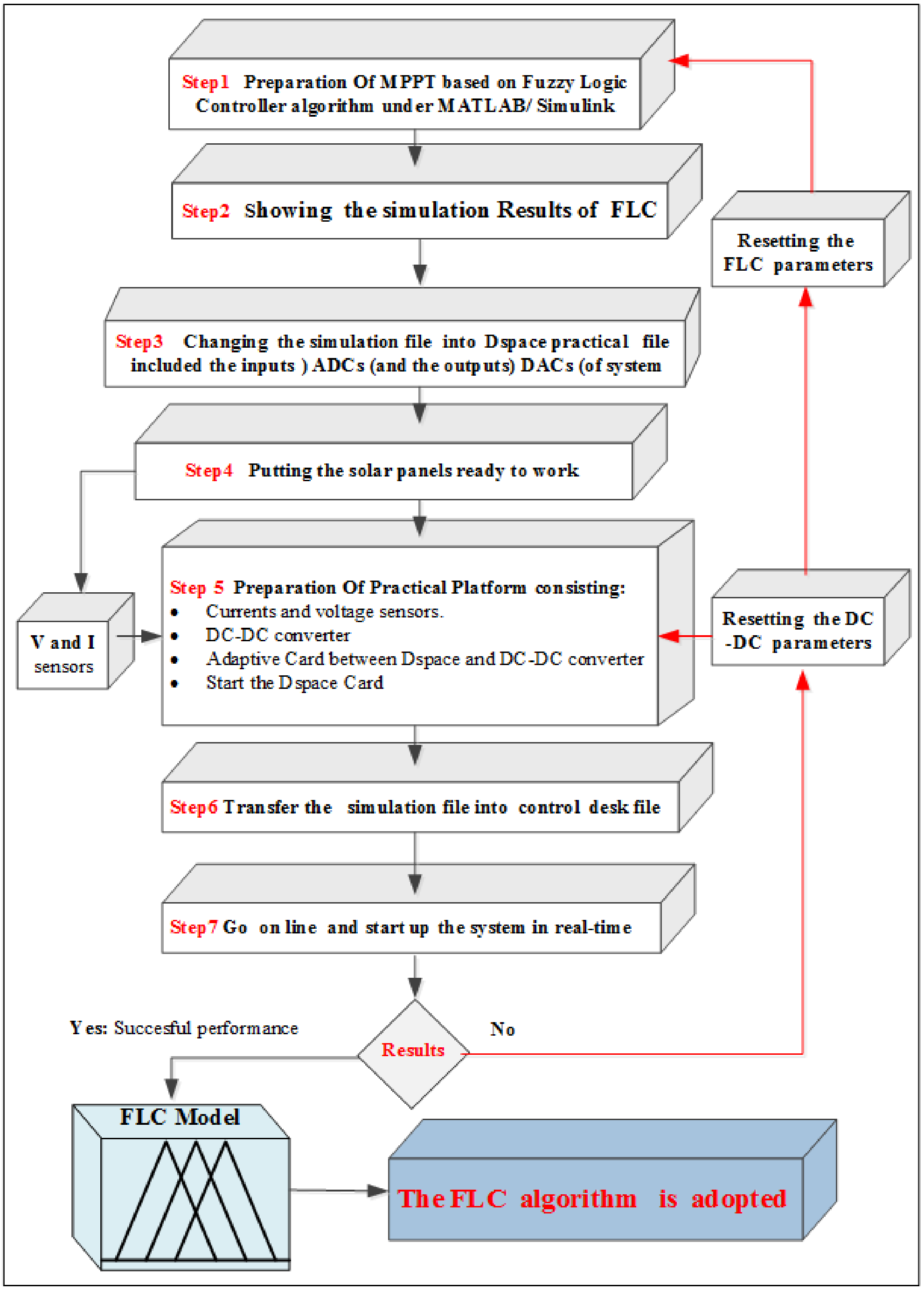

Fig. 1. Research Methodology flowchart

Figure 1 illustrates the methodology followed to generate and maintain the proposed FLC algorithm.

Step 4. Hardware Setup of PV System

The PV panels are mounted and commissioned. This task guarantees the physical system is ready for the integration of the control algorithm.

Step 5. Experimental Platform Configuration

On execution, the system performance is examined:

If the performance is found to be successful, the algorithm is verified and then implemented for practical applications.

Otherwise, two feedback loops become active:

- Initialization of DC-DC converter parameters
- Fitting and adjusting FLC parameters.

Step 6. Transfer to ControlDesk Environment

To control and monitor the real-time interface, a simulation file compatible with Dspace is sent to the Control Desk environment. The environment supports data acquisition, transmission of control signals, and performance visualization.

Step 7. Real-Time Execution and Performance Evaluation

The system is run in real-time using ControlDesk. During this phase, the FLC-based MPPT algorithm's performance is examined in terms of its ability to extract maximum power from the PV system at different operating conditions.

Step 8. Decision and Validation Cycle

After execution, the system performance is examined: If the output is acceptable, the algorithm is verified and then implemented in real-world settings. Otherwise, two feedback loops are initiated:

- Resetting of DC-DC converter parameters,
- Parameter adjustment and tuning of FLC.

Those changes are returned to the process, beginning with the required prior step (Step 1 or Step 5), thereby creating a cycle of improvement of the algorithm. Outcome The accomplishment of this methodology leads to the adoption of a verified FLC-based MPPT algorithm with the ability to operate in real-time in PV systems with enhanced energy harvesting efficiency.

The simulation file compatible with Dspace is then imported to the ControlDesk environment providing a real-time interface for system monitoring and control. The environment supports data acquisition, deployment of control signals, and performance visualization.

2.1. PV System Modeling

A. Equivalent Circuit of PV Cell

Figure 2 displays the detailed configuration of the PV cell circuit. It consists of four electrical components: a series resistance (Rs), a current source, a diode linked in parallel with the current source, and a parallel resistance (Rsh) (Premkumar et al., 2020). The diode current and the PV voltage may be determined by using the Kirchhoff Current Law (KCL) as described in the reference (Singh et al., 2013). The Rp value has a much higher magnitude when compared to the Rse value (Mujammal et al., 2024d). There are two types of installations available for the photographic system: PV stand-alone installations and solar power systems linked to the grid. Figure 2 depicts a detailed scheme of a PV cell, that involves a parallel resistor and diode. A photovoltaic module is formed by a collection of many solar cells used in a photovoltaic plant (Miles et al., 2005). These modules are then connected in series and parallel to create the photovoltaic array (Pendem and Mikkili, 2018).

The PV panel number (1 panel) defines the system's modularity, while the maximum power (200 W) represents the panel's peak output under standard test conditions. The maximum current (4.26 A) and maximum voltage (47.06 V) display the optimal operating points for reaching maximum power (Baqir and Channi, 2022). Figure 3 illustrates the realistic technical specification of solar panel parameters. The parameters of Table 1 are used according to the label provided by the solar panel manufacturer, as shown in the figure below: (Technical Specification).

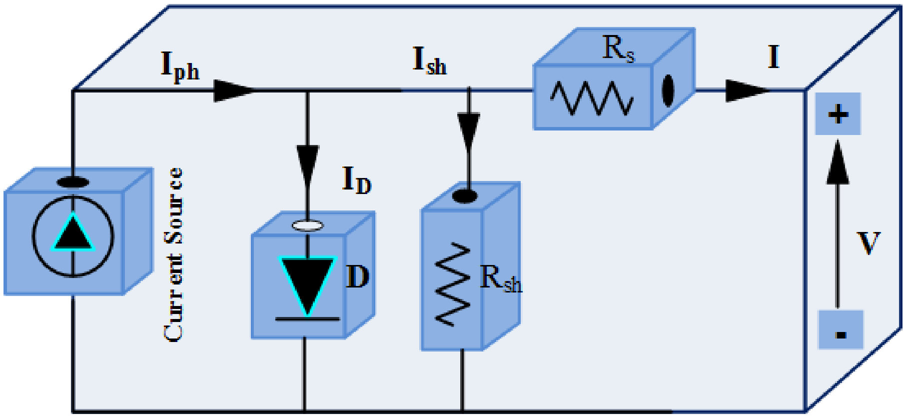

Fig. 2. Photovoltaic Cell Scheme

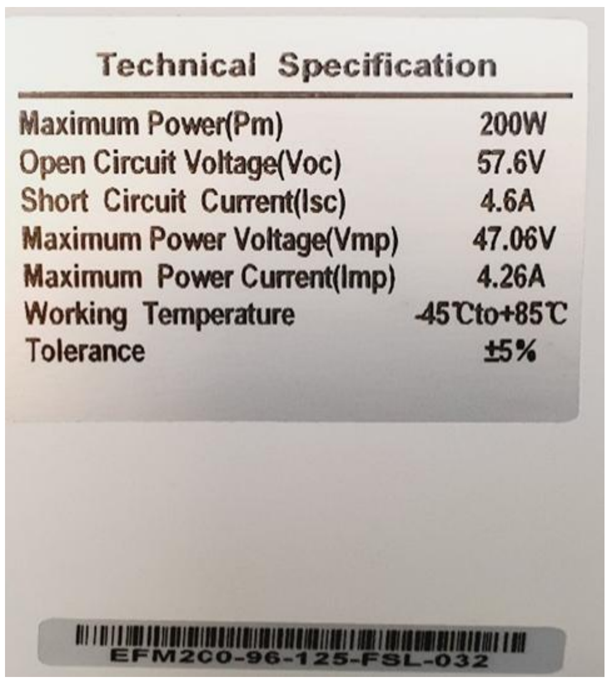

Fig. 3. Technical specification of realistic solar panel

Table 1 Specifications of the proposed pv system

Parameter	Unit and Value
PV panel Number	1 panel
Max Power	200 W
Max current	4.26 A
Max Voltage	47.06 V
Open Circuit Voltage	57.6 V
Short Circuit Current	4.6 A
Working Temperature	-45˚C to +85˚C

The mathematical relation that explains the interaction between the output voltage and current is represented via the next equations:

$$I = I_{ph} - I_D - I_{sh} \quad (1)$$

$$I_{ph} = \frac{G}{1000}[I_{sc} + \mu(T - T_r)] \quad (2)$$

$$I_D = I_0\left[\exp\left(\frac{q(V+R_sI)}{nKT}\right) - 1\right] \quad (3)$$

$$I_{sh} = \frac{V+R_sI}{R_{sh}} \quad (4)$$

$$I_0 = \frac{I_{sc}\cdot T^3\cdot \exp\left(-\frac{qE_g}{KT}\right)}{\left(\exp\left(\frac{q\cdot V_{oc}}{nKT_r}\right)-1\right)\cdot T_r^3\cdot \exp\left(-\frac{qE_{gr}}{KT_r}\right)} \quad (5)$$

$$E_g = E_{g0}\left(\frac{\alpha\cdot T^2}{\beta+T}\right) \quad (6)$$

Where q is the electron's charge (1.602 x 10-19 C), K is the Boltzmann's constant (1.381 x 10-23 J/K), N is the diode quality factor, Tc is the temperature of the PV device and, Is (A) is the current of inverse saturation (Kelvin), (Ramadan et al., 2022).

In the PV systems, fill factor, decreasing efficiency and series resistance Rs limits current discharge, while shunt resistance Rsh induces leakage currents, reducing voltage and power output. Minimum values of R_s and maximum values of R_{sh} are critical for optimal performance.

Determination of R_s and R_{sh} :By examining the current-voltage (I-V) curve of a PV cell: The incline of the I-V curve close to the short-circuit current (I_{sc}) point is affected by R_s, which uses the following formula:

$$R_s = -\left(\frac{dV}{dI}\right)_{\text{near Isc}} \quad (7)$$

While the slope of the I-V curve close to the open-circuit voltage V_{OC} is affected by R_{sh} used as follows:

$$R_{sh} = -\left(\frac{dV}{dI}\right)_{\text{near Voc}} \quad (8)$$

In a PV cell, (R_s) denotes inner resistive losses generated by the material, connections, and interconnections, significantly decreasing the output voltage, power, and efficiency under high current requirements. Ideally, R_s should be minimised to improve performance. On the other hand, (R_{sh}) accounts for leakage currents via flaws or impurities, which avoid the load and decrease the cell's output current and power. A high Rsh is desirable to reduce these losses and support the efficiency range, especially at low irradiance levels. R_s and R_{sh} affect the fill factor, efficiency, and general performance of the PV cell.

Modules in series connection are linked in series to raise the voltage while keeping the same current. A collapse in one module impacts the whole string. Modules in parallel connection are linked in parallel to boost the current while keeping the same voltage. If one module fails, the others can still function.

B. DC/DC Converter

A DC/DC converter is an apparatus that accumulates input energy to transform direct current across one voltage level into another (Salman et al., 2018). The fundamental elements used in this current subject are an input capacitor (C_1), an inductor (L), a semiconductor IGBT/Diode, a diode, and an output capacitor (C2), as shown in Figure 4. Table 3 displays the values used in boosting the converter.

- To achieve the increased output value of the DC converter shown in Figure 4, there are two operational modes:
    - When switch S is closed and switch D is open, All the input energy provided to the circuit passes through inductor L when the diode is in reverse bias. Consequently, no current passes through the diode. Rather, the input voltage applied to switch S is fed to the load, causing the output to rise.
    - When switch D is activated and switch S is deactivated, the stored energy that had accumulated in the inductor L is released back into the output, thus boosting the converter output voltage accordingly.

A comprehensive analysis was conducted on the DC/DC converter in reference (Işen, 2021; Albasheri et al., 2022).

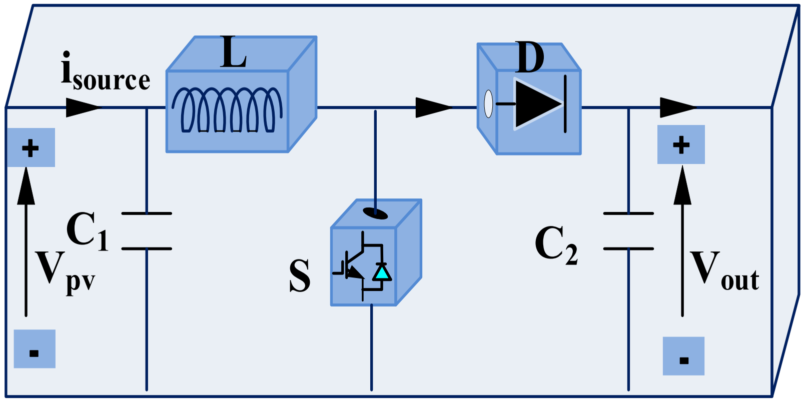

Fig. 4. Boost Converter Diagram

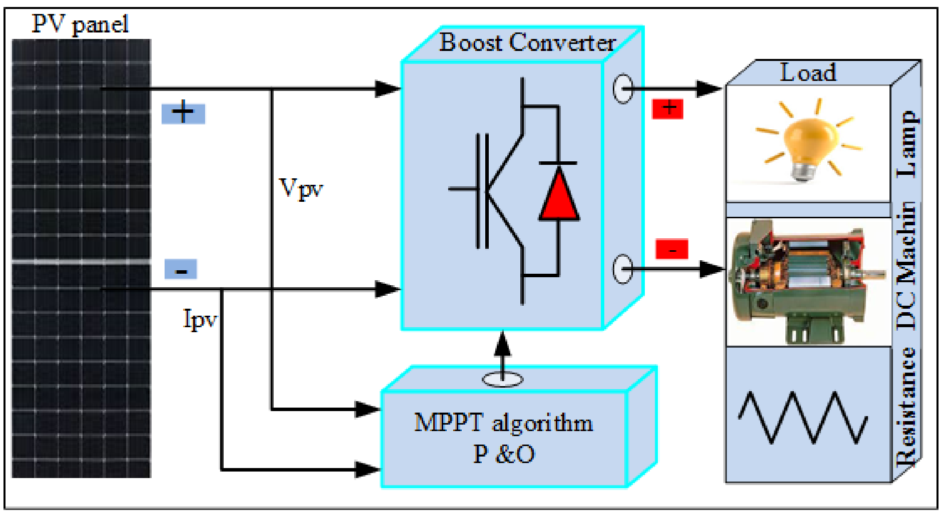

Fig. 5. General Diagram of applied system

Table 2 Specification parameters of boost converter

Parameter	Value	Unit
Output capacitor (C_2)	1100	µF
Inductor ((L)	10	mH
The input capacitor (C_1)	2000	µF

The parameters provided in Table 2 specify the basic components of the boost converter for a stable and efficient operation in the proposed photovoltaic system. The output capacitor (C2=1100 µF) is designed to minimize output voltage ripples and supply a stable DC voltage to the load. The inductor (L=10 mH) is appropriately selected to store and deliver energy effectively while minimizing current ripple during the boosting operation. Finally, the input capacitor (C1=2000 µF) is chosen to provide stabilization of the input voltage by filtering out high-frequency noise and oscillations from the photovoltaic panel. These components are designed to improve the operational efficiency of the converter, thus guaranteeing reliable energy transfer and efficient voltage regulation (Osheba et al., 2023).

Given input and output voltages of the boost converter, switching frequency fs and load current Iload, Vin=51 V, Vout= 100 V, fs= 20 kHz, Iload= 0.125 A.

Ripple current ΔI_{Load} 10%= 0.0125 A, ripple voltage ΔV_{out}=0.1 V, the parameters of the boost converter are calculated as follows:

1. Calculation of inductor L:

$$L \geq \frac{V_{in} \cdot (V_{out} - V_{in})}{\Delta I_{load} \cdot f_s \cdot V_{out}} \rightarrow L \geq \frac{51 \cdot (100 - 51)}{0.0125 \cdot 20000 \cdot 100} \rightarrow L \geq 10mH$$

2. Computation of output capacitor C2:

$$C_2 \geq \frac{I_{load}}{8 \cdot f_s \cdot \Delta V_{out}} \quad C_2 \geq \frac{0.125}{8 \cdot 20000 \cdot 0.1} \rightarrow C_2 \geq 781.25 \mu F$$

3. Computation of input capacitor C1:

$$C_1 \geq \frac{\Delta I_{load}}{4 \cdot f_s \cdot \Delta V_{in}} \rightarrow C_2 \geq \frac{0.0125}{4 \cdot 20000 \cdot 0.5} \rightarrow C_1 \geq 312.5 \quad \mu F$$

The value of 2000 μF is adequate to address the stability of input voltage and raise the filtering process (Veerachary and Kumar, 2020). The aforementioned values in Table II are realistic values that align with the experimental process in our work.

The boost converter operates in two modes (Salem et al., 2022):

- **Continuous Conduction Mode (CCM):**

The inductor current never falls to zero in this mode. This process includes two sub-phases:

  - When the switch IGBT is on, the inductor supplies energy as the current boosts linearly, and the diode is reverse-biased, isolating the load.
  - The inductor discharges while the switch is off and its stored energy to the load via the diode, keeping the output voltage higher than the input voltage (Abdulelah et al., 2023).

- **Discontinuous Conduction Mode (DCM):**

During this operation, the inductor current drops to zero for some part of the switching cycle. This leads to a distinct third phase, where no current passes across the inductor.

2.2. MPPT Strategy Based on THE FLC Algorithm

In solar power systems, (MPPT) is a key concept as it constitutes the foundation of maximizing the energy output of solar panels. The current research proposes an MPPT strategy founded on an advanced FLC to enhance the operating efficiency of photovoltaic (PV) systems. Figure 5 illustrates the development process of the FLC algorithm utilizing an intricate flowchart.

The (MPPT) concept is a critical challenge in the area of solar energy systems since it is tasked with the maximization of the generation of solar energy (Ali et al., 2023; Osman et al., 2021). In this study, an MPPT system with a FLC is employed to enhance the operation of the photovoltaic (PV) system. Figure 6 presents a flowchart illustrating the design process associated with the FLC method.

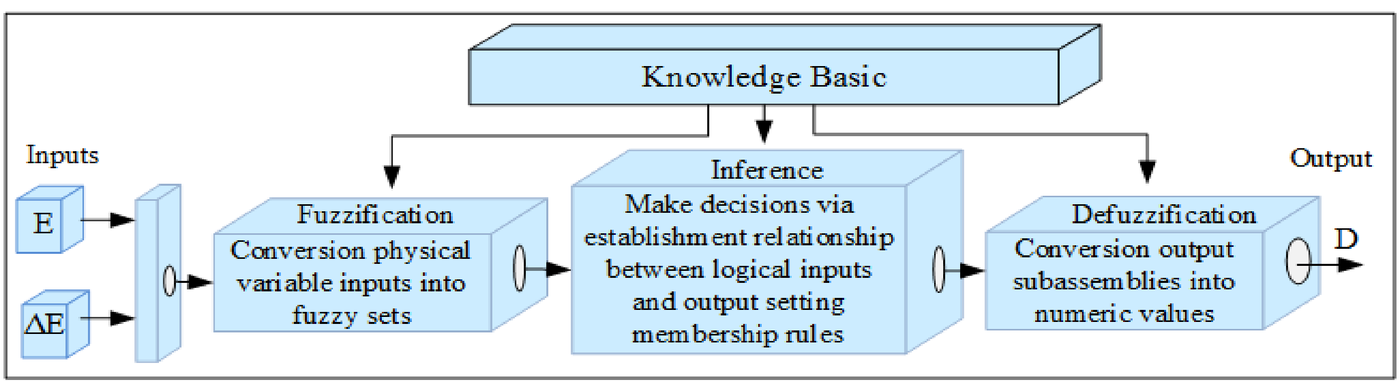

Fig. 6. Fuzzy Logic Formation Stages

Conventional MPPT algorithms face considerable challenges in successfully coping with energy losses under steady-state conditions, along with showing poor dynamic responsiveness when subjected to abrupt changes in irradiance and temperature (Gernaat et al., 2021). Overcoming these challenges requires the exploration of an advanced algorithm that can rectify serious shortcomings while providing a rapid adaptive response to sudden changes in environmental conditions. Figure 7 depicts the (FLC) flowchart together with its two inputs, namely the error (E), the derived error (ΔE), and its output, the duty cycle (D).

2.3. Proposed FLC Algorithm Design

By the scenario of FLC algorithm, the proposed MPPT to design through six-steps procedure of fuzzy design mechanism:

Define Input and Output Variables: The two input variables (Error and derivate Error) are specified as follows:

$$\mathrm{E_p} = A = P^* - \mathrm{P_{mes}} \tag{7}$$

$$\Delta\mathrm{E_p} = \Delta\mathrm{E_p}(\mathrm{k}) - \Delta\mathrm{E_p}(\mathrm{k}-1) \tag{8}$$

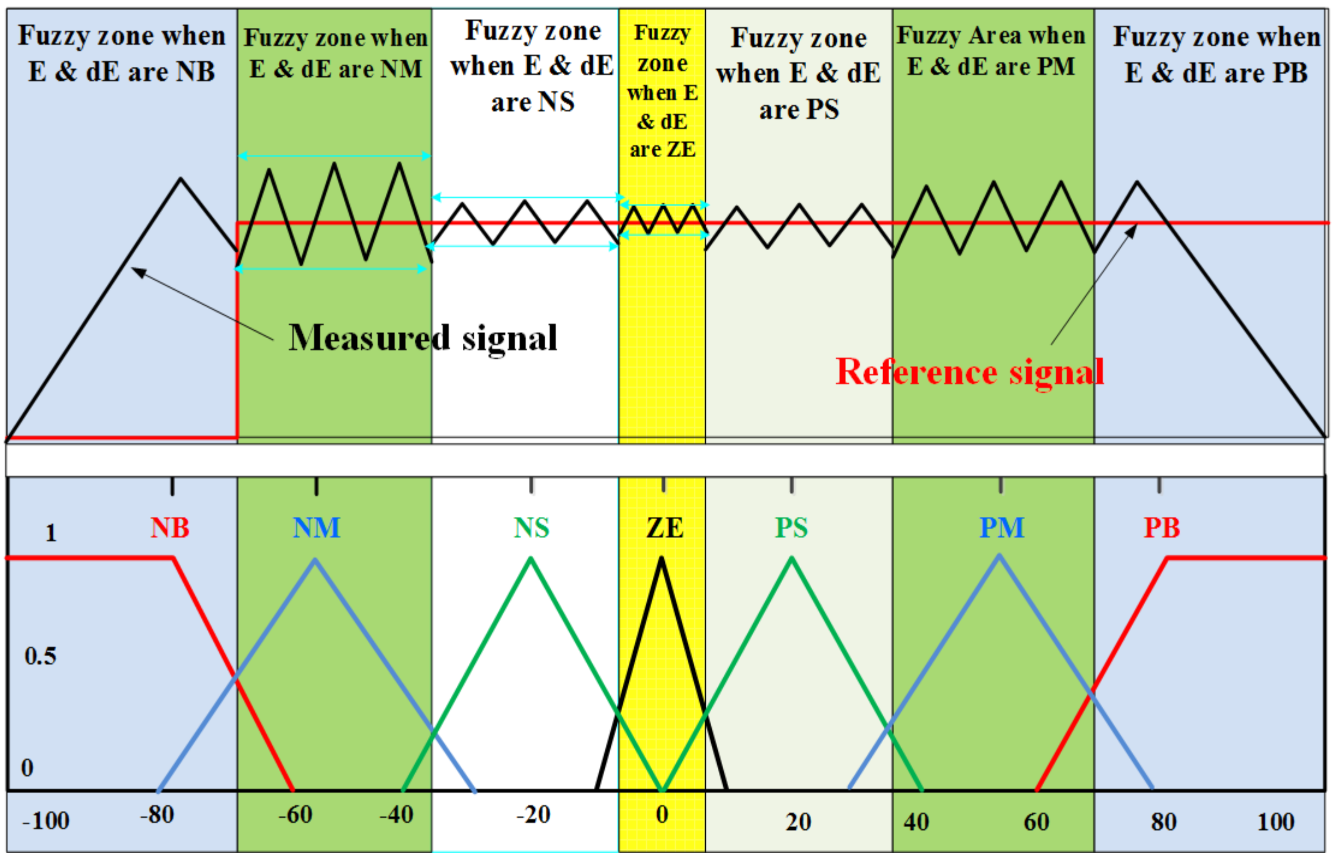

Fig. 7. Design system of Fuzzy logic controller

The nature of ΔE corresponds with rule-based fuzzy logic (if-then), enabling intuitive and efficient control. Therefore, these inputs supply a proportion of accuracy, responsiveness, and computational efficiency for a robust MPPT method.

Error is the deviation between the reference power and actual power, as determined by how fast the system is shifting from the (MPP). Through the derivative error, the rate of change of error with time is captured. The controlled output by duty cycle (D), placing the operating point at the MPP while adjust the PWM signal.

For the FLC algorithm, the error (E) & derivative error (ΔE) are selected inputs to comprehensively manage the system's dynamics and operational conditions. The deviation from the MPP denotes by Error (E), providing essential feedback for corrective actions, while ΔE reflects the rate of change of E, enabling predictive control and quicker convergence. This combination provides effective tracking under dynamic conditions, reduces power loss due to fluctuations, and stops overshooting. Besides, E and ΔE together improve adaptability to the nonlinear attributes of photovoltaic (PV) systems and enhance response to quick environmental variations.

Fuzzy Inputs and Output

The fuzzification methodology includes defining the input and output variables into linguistic terms. In our work, the linguistic variables have been simplified as follows: NB for Negative Big, NM for Negative Moyne, NS for Negative Small, ZE for Zone Zero, PB for Positive Big, PM for Positive Moyne, and PS for Positive Small as shown in Figure 7. Triangular membership function shapes are assigned to each linguistic term to describe their degree of membership. The triangular functions translate the crisp input values into fuzzy sets, authorizing the system to operate with on nonlinearities and uncertainties.

Construct the Rule Base

The input & output relationship eminently ties through the rule configuration which is the most significant process of the FLC algorithm. Through the field knowledge and the system's arrangement, the rules are finalized. For example, the duty cycle needs to rise to move towards MPP while the error is mainly positive. Conversely, when the error is predominantly negative, the duty cycle needs to decline to minimize overshoot. If the E is small and the dE converges to zero, the duty cycle is stable, the system is near the MPP, as shown in Figure 7.

Defuzzification of the Output

The FLC system transforms the fuzzy outputs derived from the rule base into a crisp value for the duty cycle via a technique called defuzzification. Standard techniques contain the centroid of area (COA), where the output value is defined as the center of gravity of the aggregated fuzzy set, or the bisector of area (BOA), which separates the area of the fuzzy set into two equal parts. This step ensures that the output is actionable and can be used for the PWM in the MPPT.

Simulate and Optimize

MATLAB/Simulink supplies an intuitive graphical interface and an extensive library of pre-built blocks, such as fuzzy logic controllers. Figure 8 presents the maintenance process of the proposed FLC method for (MPPT).

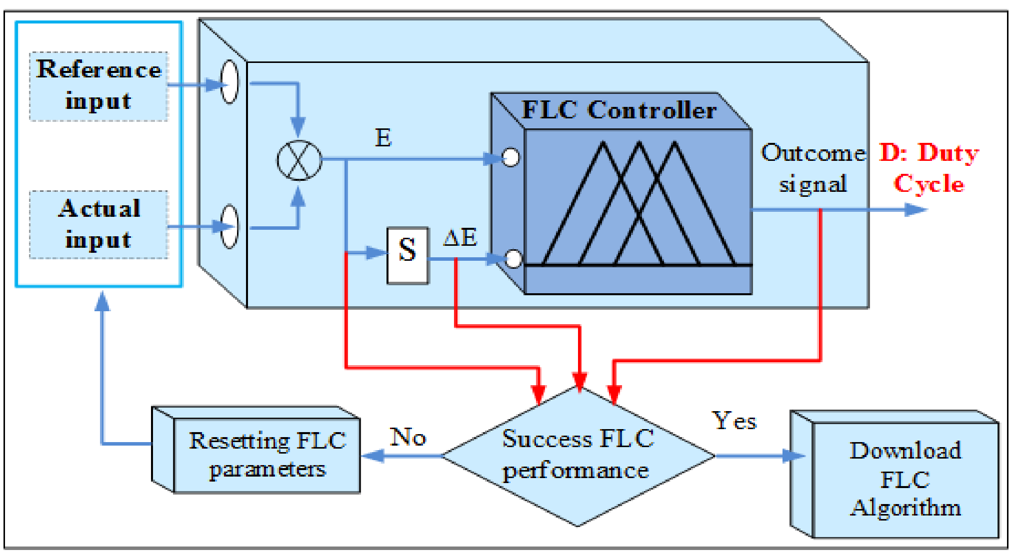

Fig. 8. Fuzzy Logic Components

Additionally, to the management of dynamic simulations, MATLAB/Simulink is an eminent environment, these are very significant factor for assessing the performance of MPPT under varying circumstances like temperature conditions and solar irradiance. For in-depth investigation of system performance, the MATLAB/Simulink's robust analytic tools permit advanced visualization.

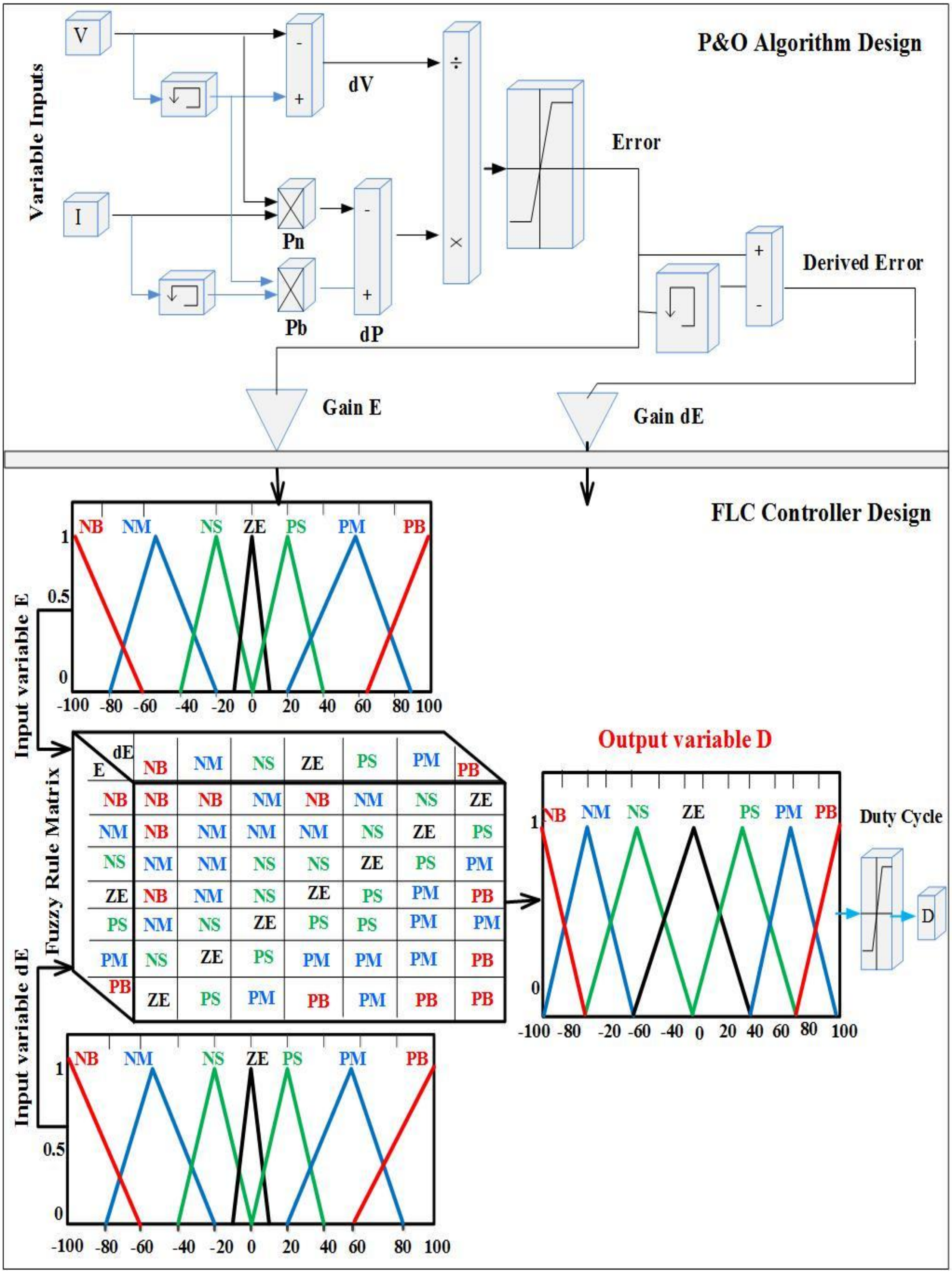

Fig. 9. MPPT based on the FLC via MATLAB/Simulink Software

It is necessary to introduce linguistic variables into the framework of fuzzy logic control for several reasons (Daradkeh and Tvoroshenko, 2020). Firstly, it enables the quantification of qualitative human knowledge and reasoning in mathematical terms, thereby making the control system more interpretable and accessible. Linguistic variables also enable the handling of imprecise and ambiguous information, which is a frequent phenomenon in practical applications, and therefore further prepares the system to tackle varied situations.

2.4. Scalability of the FLC Algorithm

The suggested (FLC) algorithm portrays a degree of scalability that renders it suitable for the different designs of (PV) systems targeted at large-scale applications. In the framework of small-scale designs, the algorithm operates a compact rule and a small membership function set to achieve the control operation with minimal computational cost. The FLC framework enables decentralized management, allowing multiple FLC units to be utilized in parallel for controlling separate sections within the PV system. This involves load sharing of computation and an improvement in the system's scalability, without compromising stability or response time.

One of the biggest challenges is that it requires more computational complexity compared to traditional methods like P&O or IC methods. There are more computations involved with the fuzzy inference process and defuzzification processes, which would be prohibitive for low-cost or low-capability microcontrollers. Additionally, the performance of the FLC is very sensitive to the rule base and membership function setting. A satisfactory rule set may require expertise and even be a time-consuming task, with inefficiently chosen settings reducing efficiency.

Moreover, FLC systems need to be tuned periodically to adjust for varying system conditions or aged PV modules, adding up to maintenance costs. Despite these setbacks, advancements in computational technologies and adaptive tuning methods restart to improve the viability of FLC to make it feasible for a multitude of solar applications.

3. SIMULATION RESULTS

MATLAB/Simulink has a friendly graphical user interface and an extensive library of pre-developed blocks, which even include fuzzy logic controllers. Moreover, MATLAB/Simulink is well-suited for dynamic simulations, which are necessary to evaluate MPPT performance under variable solar irradiance and temperature conditions. Its robust analytic tools and advanced visualization abilities permit for in-depth investigation of system performance.

Additionally, MATLAB's toolbox, which includes the Fuzzy Logic Toolbox and Optimization Toolbox, enables the design, optimization, and fine-tuning of fuzzy rules and membership functions. These features of MATLAB/Simulink are a highly reliable and adaptable choice for designing and validating MPPT.

Figure 10 A and B illustrate the MPPT area. When preserving the MPPT zone, the power, current and maximum points of voltage are increased by the efficacy of the FLC-MPPT algorithm. Figs. 12 & 13 demonstrate & correlate the simulation outputs between projected FLC-algorithm and the conventional P&O method. The proposed FLC algorithm achieved excellent performance, free of significant ripples, which proves the effectiveness of the FLC algorithm.

Table 3. Specification Parameters of Boost Converter

Parameter	FLC Performance	P&O Performance
Irradiation Response	Quick adaptation at t=4s (900 W/m²) and t=7s (1000 W/m²).	Slower adaptation with more oscillations.
Output Voltage	~275 V (steady-state) with minimal oscillations.	~225 V (steady-state) with larger oscillations.
Output Power	~245 W at t=7s (1000 W/m²).	~175 W at t=7s (1000 W/m²).
Transient Oscillations	Oscillations reduced to ~0.5% during transitions.	Oscillations up to ~2% during transitions.
Efficiency	~98%	~95%

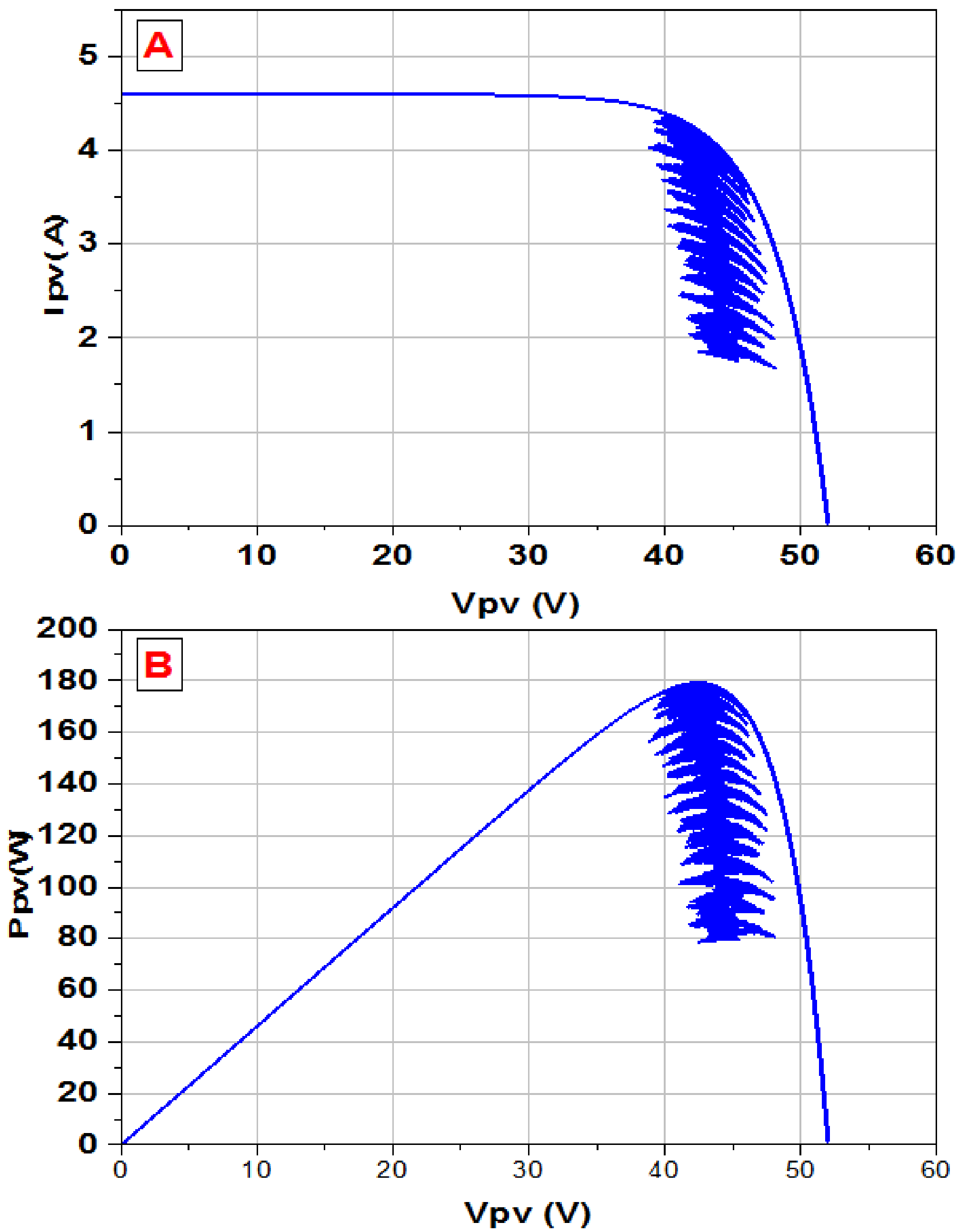

Fig. 10. Characteristic curves P-V of MPPT technique

At t = 4s, the irradiation reduces to 900 W/m², resulting in a corresponding adjustment in the output voltage and power of the boost converter. Also, at t = 7s, the irradiation rises to 1000 W/m² as shown in Figure 11. The system responds effectively by increasing the voltage and power levels of the boost converter. These quick and precise reactions to varying irradiation states indicate the FLC's capacity to track the (MPP) efficiently.

The FLC's adaptability stems from its ability to manage non-linear behaviours and dynamic changes in the PV system. Unlike conventional MPPT algorithms, such as (P&O) or (IC), the FLC does not depend on fixed step sizes or linear decision-making. Instead, it employs a rule-based system to analyze changes in inputs (e.g., changes in irradiation) and outputs (e.g., voltage and power), allowing smoother transitions and quicker convergence to the MPP. Moreover, the FLC improves system performance by minimizing oscillations about the MPP and lowering energy losses during transient states (Guerri). This ensures that the system is utilized optimally, even under challenging conditions, such as rapidly varying irradiation levels.

The sensitivity analysis emphasizes the robustness of FLC under extreme climatic conditions. Although there is a small degradation in performance, the controller restarts to operate effectively, keeping stability, efficiency, and adaptability. These outcomes prove that the FLC is well-suited for deployment in real-world PV systems where climatic variations are common.

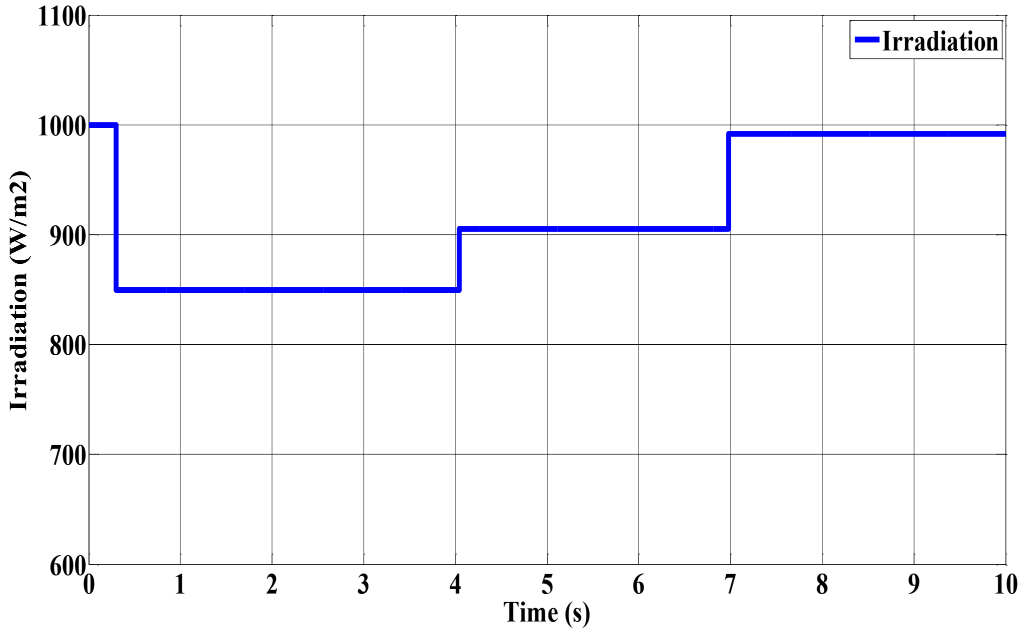

Fig. 11. Irradiation profile for PV system

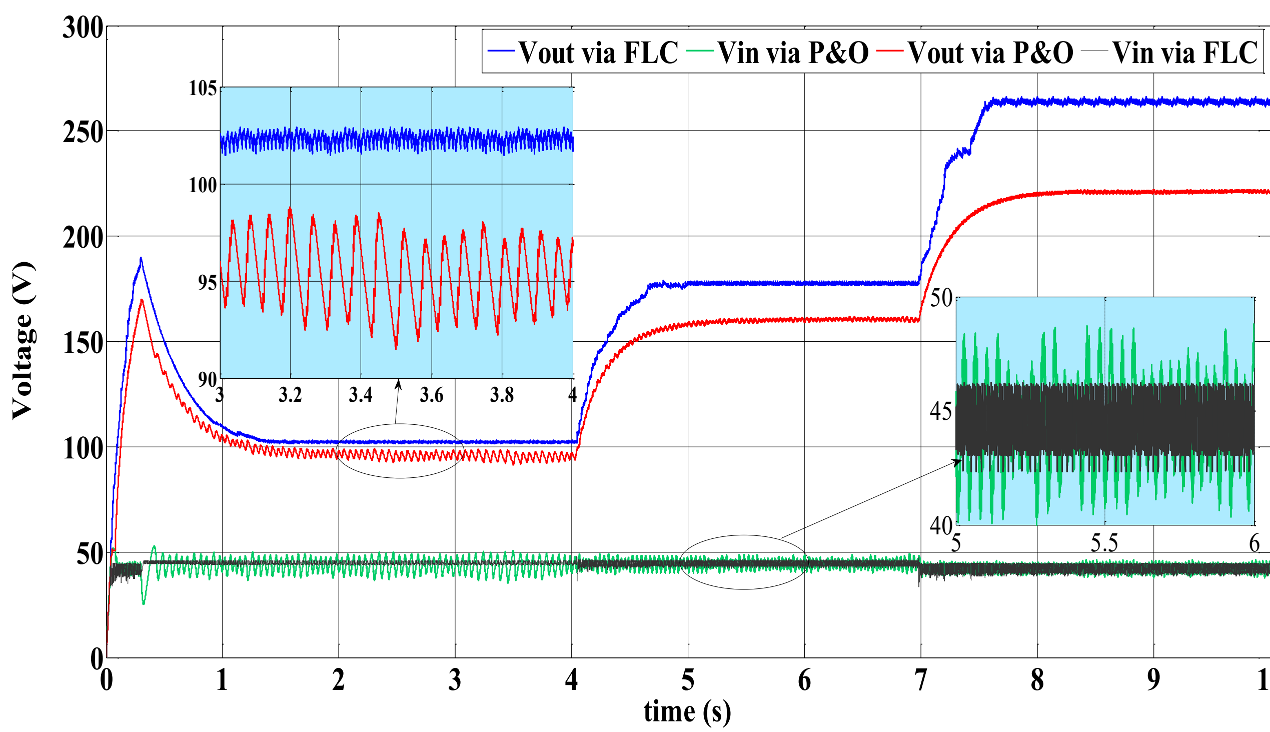

Fig. 12. Boost converter Input and output voltages.

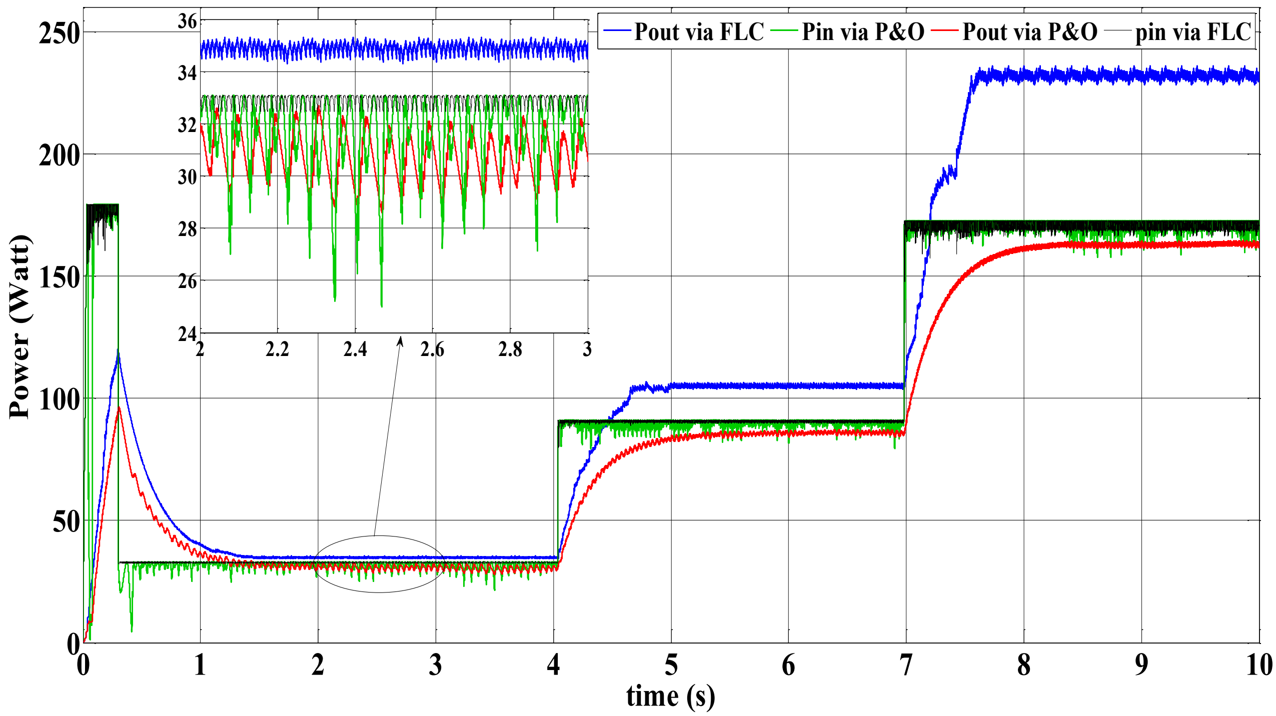

Fig. 13. Input and output powers of the boost converter

Equipment Calibration

Solar Panel: Under standard test conditions (STC), the solar panel was tested to provide proper output characteristics, as shown in Figure 13.

Current and Voltage Sensors: The current and voltage sensors were calibrated using a reference multimeter (with an accuracy of ±0.05 %) to ensure accurate voltage and current measurements during experiments.

Digital multimeters were calibrated to measure the boost converter's input and output voltages and currents. These devices conform to the IEC 61010 standard for measurement equipment.

4. EXPERIMENTAL RESULT

To assess the results of the algorithm we have developed and showcase the usefulness of the outcomes, we carried out a three-minute experimental verification test using MATLAB software and DSpace 1103 hardware. Figure 14 illustrates the fundamental equipment and instruments utilized on the experimental platform.

***Oscilloscope*:**

The oscilloscope was calibrated by a reference signal generator to ensure correct waveform visualisation of the boost converter's input and output voltages.

dSPACE 1103 Controller:

The dSPACE system was configured and calibrated to actually communicate with the adaptive card, providing precise real-time data acquisition and control.

Test Conditions:

The experiments were executed in a controlled laboratory platform, with ambient temperature and irradiation. Resistive and capacitive loads were used to simulate grid and battery storage integration. The loads were adjusted to analyze system performance under different operating conditions.

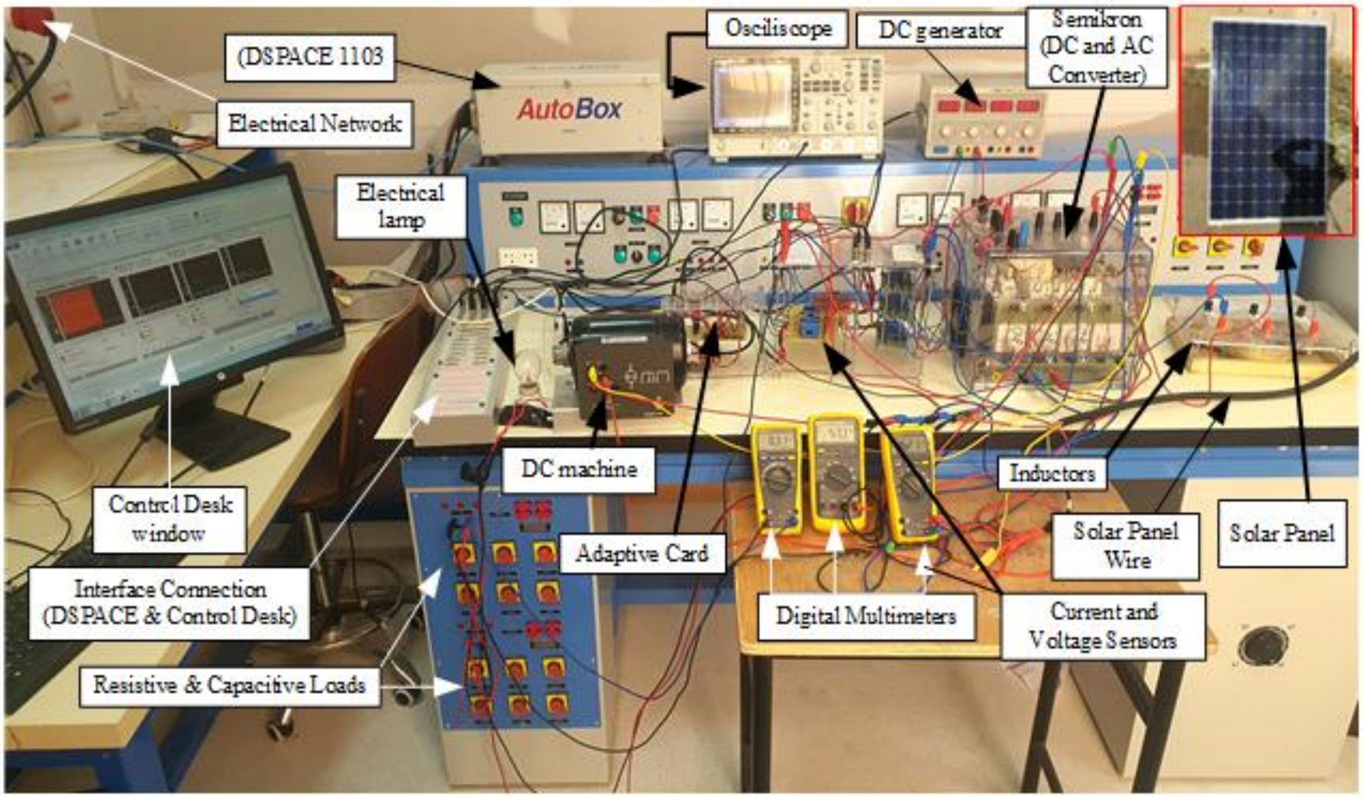

Fig. 14. Experimental Platform of Test

A. Experimental Results of MPPT Under Constant Resistive Load

The experiment included implementing the Maximum Power Point Tracking (MPPT) method using Fuzzy Logic Control (FLC) with a resistive load that remained constant throughout the experiment. Figures 15, 16, and 17 show the results of the proposed Maximum Power Point Tracking (MPPT) method for the voltage output of the solar panel (Vpv), the voltage output of the boost converter, and the power output of the boost converter, respectively. The FLC exhibited a smoother and less oscillatory performance, attributed to its capacity to effectively adjust to abrupt changes in air conditions.

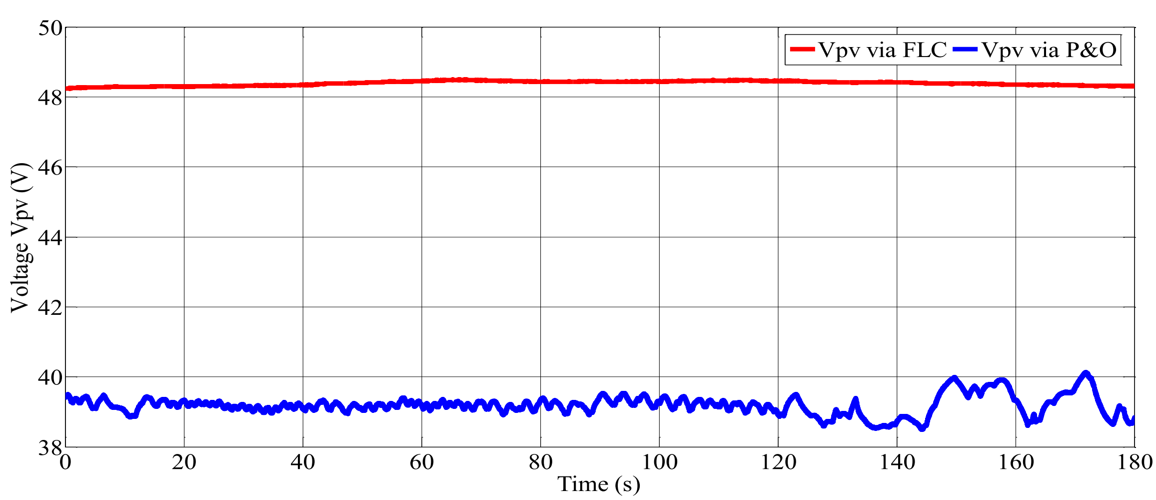

Fig. 15. Solar panel output voltage

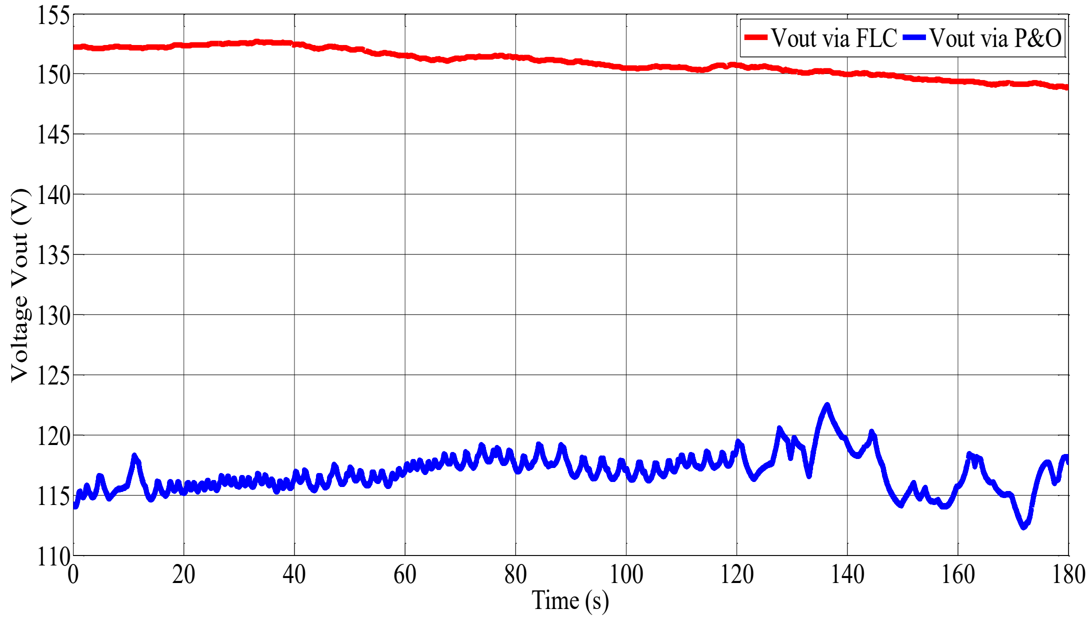

Fig. 16. Boost Converter Output Voltage Vout (V)

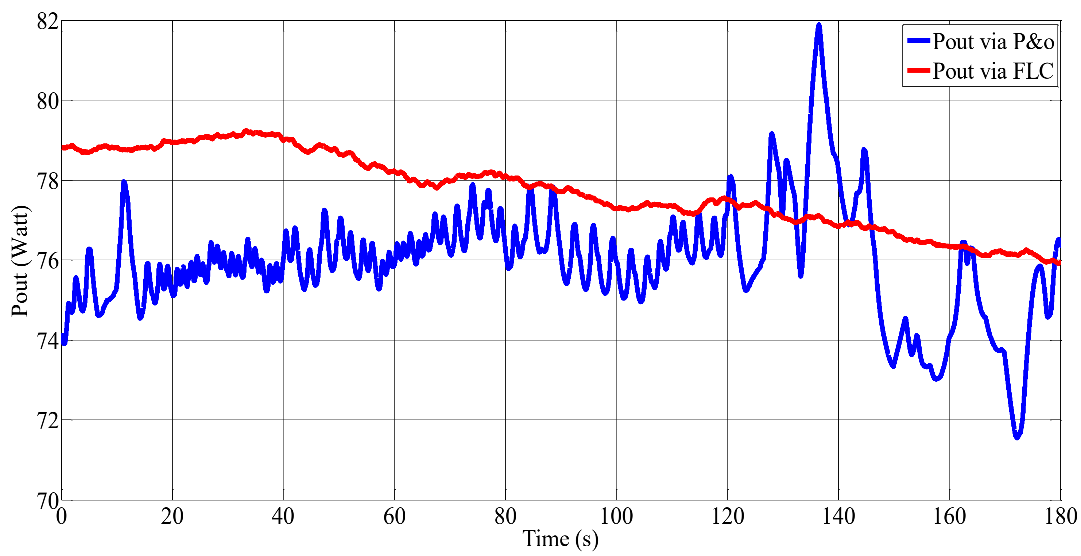

Fig. 17. Boost Converter Output Power P(W)

B. MPPT Performance of FLC Algorithms Under Changeable Resistive Load

This experiment was conducted to evaluate the performance of the MPPT-FLC algorithm under various DC resistive load conditions at two time periods, specifically at t = 60 s and t = 120 s. The main goal of this experimental design is to evidence the speedy responsiveness of the MPPT-FLC algorithm under various DC resistive load conditions.

The boost converter's input-voltage, output-voltage and the output-power demonstrated in the Figs. 18, 19 & 20 respectively. As explained in Fig. 21, the study revealed that, the boost converter of FLC algorithm had enhanced efficacy which is around 0.83.

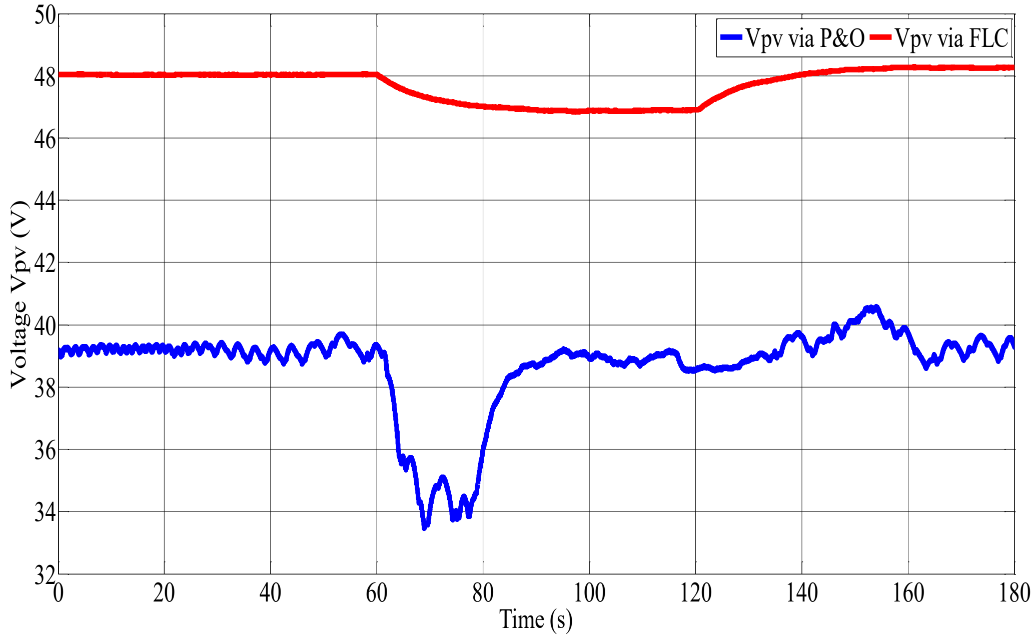

Fig. 18. Boost Converter input Voltage with variable DC load.

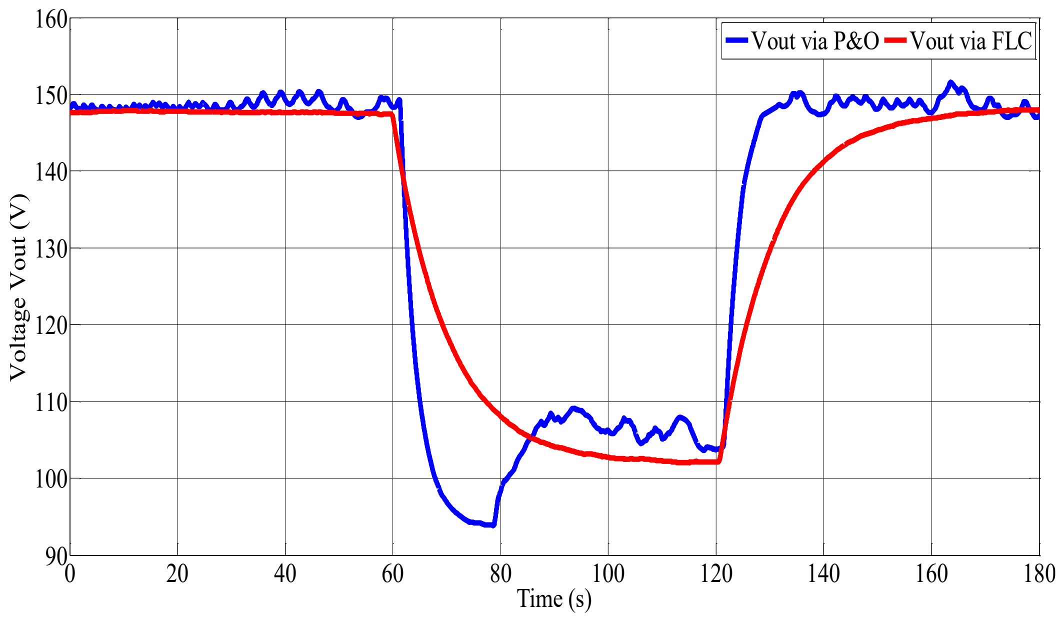

Fig. 19. Boost Converter Output Voltage with variable DC load.

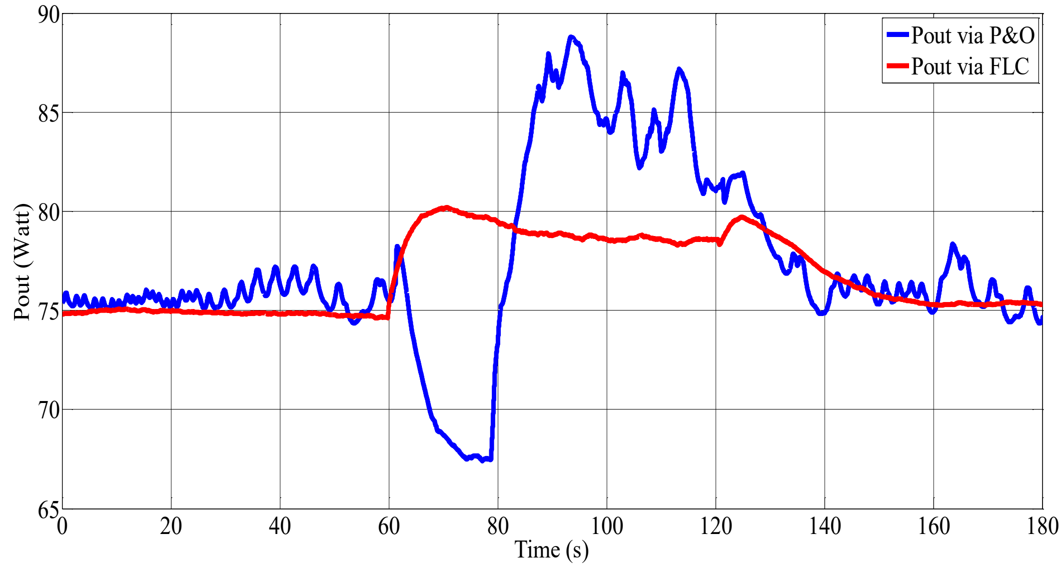

Fig. 20. Boost Converter output power with variable DC load

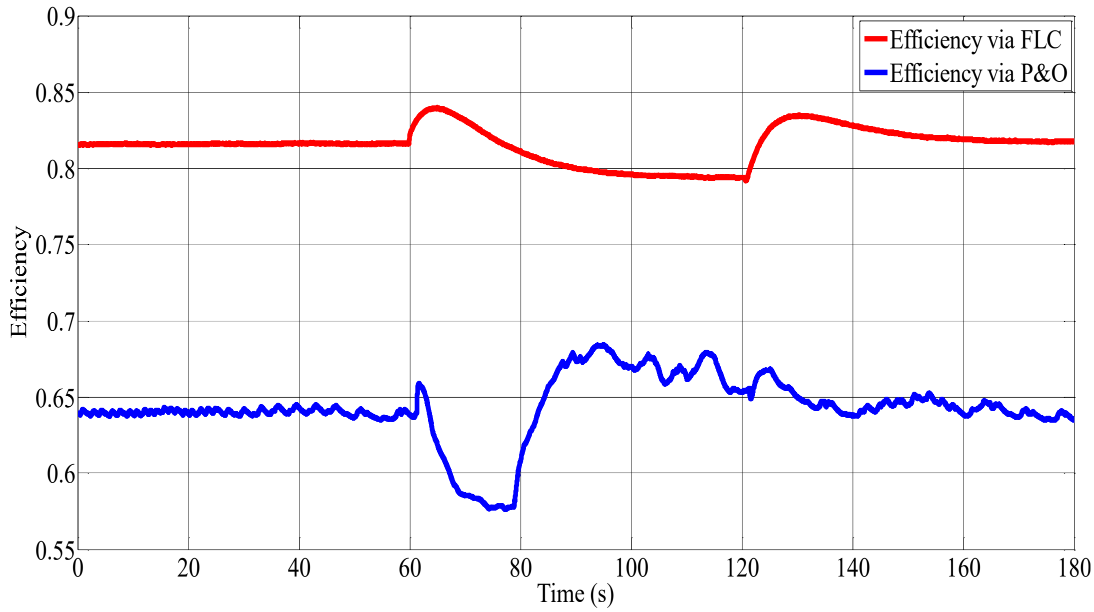

Fig. 21. Boost Converter efficiency

C. MPPT Strategy Implementation Under DC Machine Load

This experiment was conducted to evaluate the performance of the MPPT-FLC algorithm under fluctuating DC resistive load conditions at two different time intervals: t = 60s and t = 120s. The objective of this experiment is to demonstrate the rapid responsiveness of the proposed approach under varying levels of workload.

Figures 22, 23, and 24 depict the results of the input, output voltage, and power of the boost converter, respectively. It is worth mentioning that the FLC algorithm demonstrated higher efficiency, as shown in Fig. 25, where the efficiency of the proposed method is approximately 0.83.

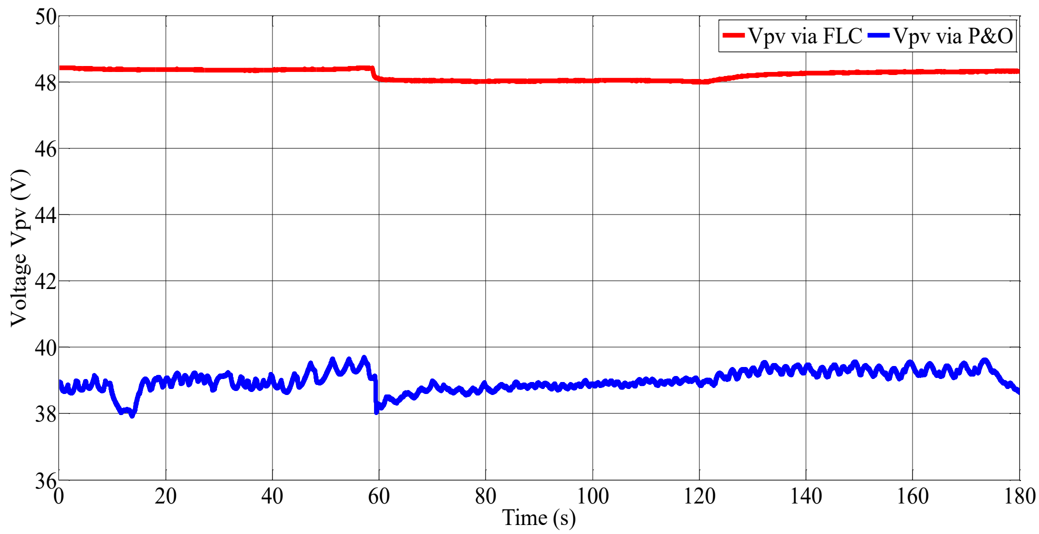

Fig. 22. Input voltage of boost converter

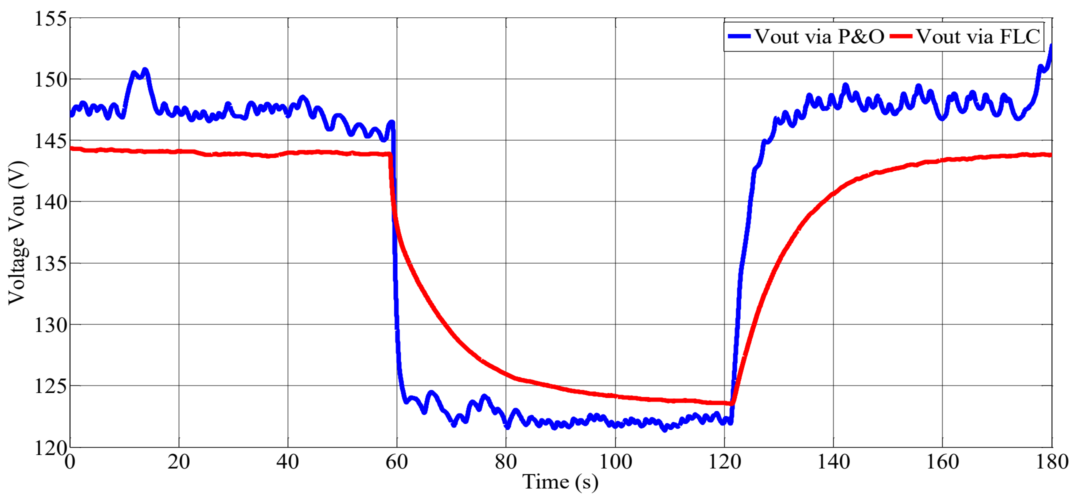

Fig. 23. Boost Converter Output Voltage

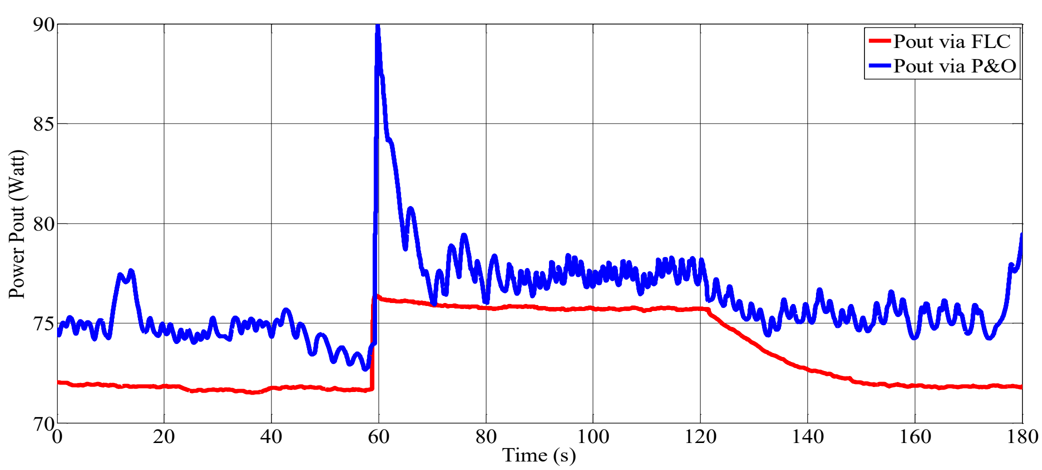

Fig. 24. Boost Converter Output Power with DC machine load

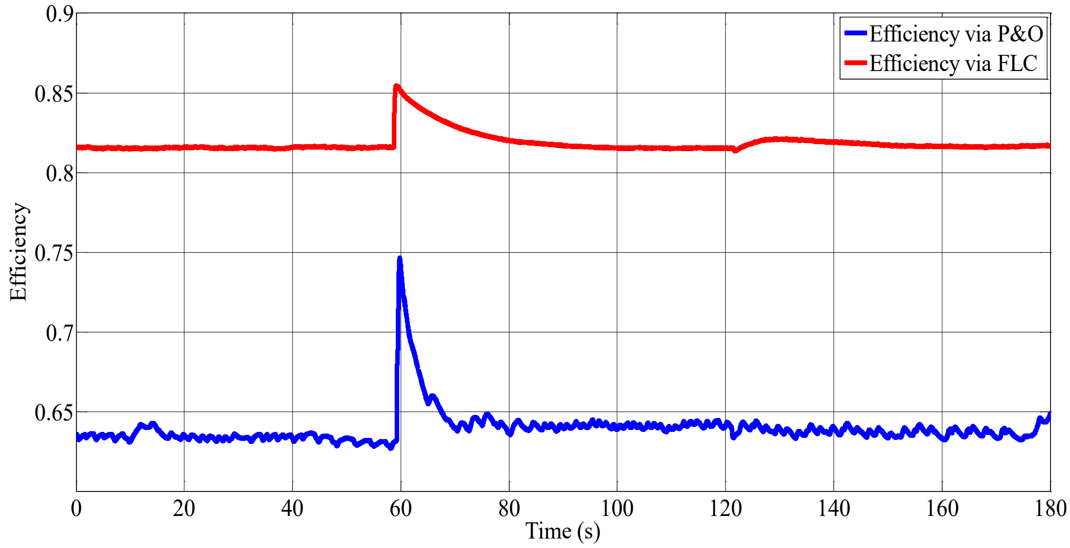

Fig. 25. Boost Converter efficiency with DC machine load

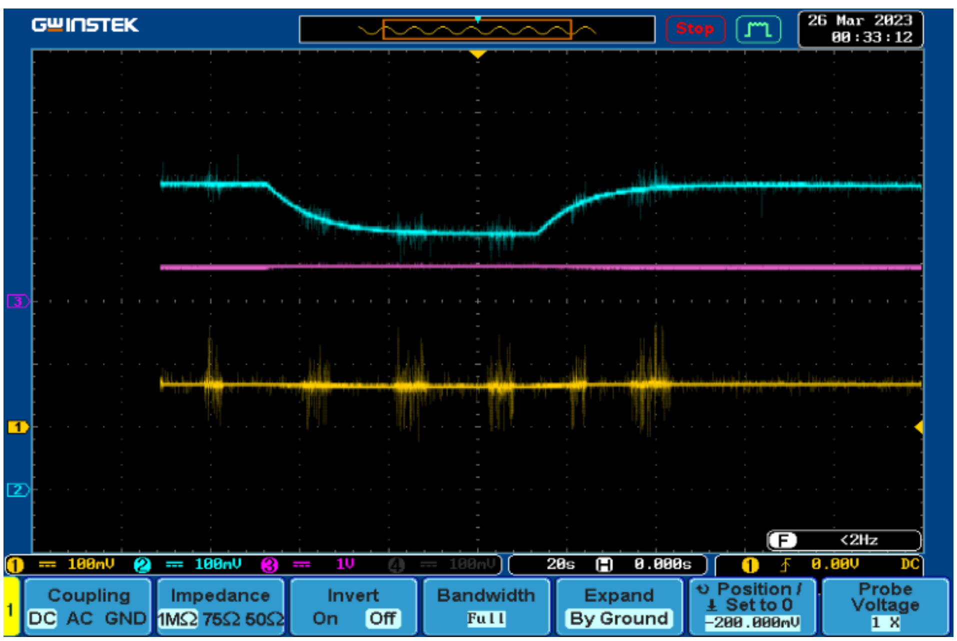

Fig. 26. Experimental Outcome of MPPT via FLC Algorithm

Fig. 26 presents experimental findings of the proposed MPPT algorithm. It can be seen that the FLC has a fast response to the sudden variations of load with high efficiency.

Key points from the experimental validation include:

- Real-time Implementation: The FLC-based MPPT algorithm was implemented in real-time, demonstrating its practical applicability.
- Response Time: The system's response to changes in atmospheric conditions, such as irradiation and temperature, was rapid and efficient.
- Stability and Accuracy: Maximum Power Point (MPP) & minimizing energy loss are accurately and steadily tracked by the proposed algorithm.

- Adaptability: The load variations in diverse environmental conditions & optimal performances are well maintained through efficiently adopted and improved FLC algorithm design.
- Hardware Integration: Successful integration with DSpace 1103 hardware showcased the algorithm's robustness and ease of implementation in real-world scenarios.

There are many limitations of the experimental setup that can impact the validity and generalizability of the results. Environmental conditions in the controlled setup may not precisely replicate real-world variation, e.g., temperatures or grid disturbances. The generation of measurement inaccuracies can occur while limiting the tools usages, for example - potential calibration faults and sensor precision. The small-scale measurements may not be able to operate in challenging environments and not investigate topics of integration when imposed the further limitations by the scale and design size.

5. DISCUSSION AND ANALYSIS

Long-Term Stable Performance:

Even the condition of occurrence of variations in load and also in the diverse environmental conditions like temperature variations and irradiation, the executed FLC-based MPPT-algorithmic method in the current research was demonstrated the consistency and steadiness in the tracking of t (MPP). This equilibrium and stability maximize the extraction of power and minimize the losses of energy.

Rapid Adaptation to Load Variation:

Tests with various resistive and DC machine loads demonstrated that the algorithm adjusted quickly to changes, producing smooth voltage and power outputs with minimal oscillations. The quick response highlights the algorithm's ability to handle dynamic functional conditions effectively. The algorithm was run with both fixed and changing resistive loads, as well as a dynamic DC machine load.

With variable Resistive Load:

For the validation of minimal disturbance in voltage outputs and in power like load variations at =60 t=60s and =120 t=120s, the rapid response was gained from FLC-based MPPT-algorithm. Consequently the algorithm's adaptability for dynamic environmental conditions was revealed. The system unveiled efficient adaptation without revealing the significant oscillations while the DC machine load addition and removal. This conditions explains the capability of MPPT-algorithm for the sustainable performance when the loads in complex & dynamic condition.

Efficiency Maintenance:

The research output specify that the FLC-algorithm constantly upheld a high degree of efficiency, approximately 0.83, regardless of load changes or test duration. Such consistency reflects its capability to sustain performance over extended time intervals.

Resistance to Atmospheric Changes:

The algorithm's capacity to absorb sudden atmospheric changes, including variations in irradiation levels, enabled stable power generation and reduced susceptibility to oscillations that might otherwise render the system unreliable.

Reduction in Oscillations:

The most impressive segment of results highlighted in the experiments was the reduction in oscillations during tracking MPP. Soft operation is a result of the fuzzy logic controller's capacity to use linguistic rules and continuous adjustment of control parameters, which resist sudden changes and jittering typical of traditional MPPT methods.

The suggested FLC-based MPPT algorithm reduces system costs and power losses by effectively tracking the Maximum Power Point (MPP), thereby minimizing power loss under varying conditions. Its simple and robust structure lowers maintenance requirements and enables the utilization of low-cost hardware, enhancing the overall economic viability of solar systems. The suggested FLC-based MPPT system is economically viable due to its simple design and efficient implementation. The technology reduces operating and installation costs by minimizing energy losses and enabling the use of low-cost components. Furthermore, its higher performance in a range of climatic conditions minimizes maintenance and downtime, hence making it less expensive for large-scale solar deployment and grid applications.

The comparison of MPPT algorithms reflects the aggressive transition from conventional to new intelligent techniques for improving the performance of photovoltaic (PV) systems, as shown in Table 4. Traditional algorithms such as P&O, IC, and Fractional Open Circuit Voltage (FOCV) are still being utilized due to their simplicity and reduced cost. However, their limitations, such as oscillations around the MPP, inferior dynamic tracking, as well as their sensitivity to external variations, limit their efficiency. These conventional techniques normally achieve efficiencies of 0.60%–0.72%, as highlighted in Esram and Chapman, (2007) and Femia et al., (2024). To overcome these limitations, recent studies have focused on AI-based MPPT techniques. (FLC)-Based MPPT, as illustrated in the suggested study, shows better tracking precision with a quick response time of under 3 milliseconds and efficiency of 0.83%. Neural network-based approaches also enhance precision and flexibility, achieving an efficiency rate of up to 0.88%, as shown by (Wang et al., 2018).

More recently, in positive dynamic environments, metaheuristic and bio-inspired optimization algorithms have achieved & contributed in traction for global MPP tracking. Few techniques have showed efficacies very adjacent to or exceeding 0.90%, for example (i) Ant Colony Optimization (ACO) (Khalid et al., 2024); (ii) Grey Wolf Optimization (GWO) (Hoseinzadeh et al., 2023); and (iii) Whale Optimization Algorithm (WOA) (Erixno et al., 2024).

Table 4 key matrix correlation between the proposed Fuzzy-Logic-Controller and other conventional MPPT-algorithm

Characteristics	**Fuzzy Logic Controller** (*Ref:* Kumar & Balakrishna, 2024)	**Perturbation and Observation** (*Ref:* Seeling-Hochmuth, 1997)	**Incremental Conductance** (*Ref:* Pradhan et al., 2022)	**Particle Swarm Optimization** (*Ref:* Mohandes, 2012)	**Neural - Network** (*Ref:* Villegas-Mier et al., 2021)
Adaptability	For diverse environmental conditions, its Highly adaptable	Limited	Moderate	Highly	Extremely adaptable
Response to Dynamics	For rapid environmental changes, it gives Fast-response	Slower	Moderate	Fast response	fast
Partial Shading	Effective	Struggles	Struggles	Effective	Excellent
Convergence Speed	Fast	Moderate	Moderate	High	High
Steady-State Oscillation	highly stable	High	Low	Low	Stable
Complexity	Moderate to high	Low	Moderate	High	high
Efficiency	Superior-tracking efficiency	Moderate	Moderate	High	high

6. CONCLUSION

Through the operation of MATLAB/Simulink software & functioning of Dspace 1103 hardware, the novelty and real-time application of FLC algorithm based MPPT-method has been comprehended in our research. The efficient and rapid response revealed, resolved and concluded through FLC algorithm based MPPT-method and effective maximum power point tracking, even during changes in loads and uneven atmospheric conditions, such as fluctuations in irradiation and temperature. In addition to this, smooth and stable behaviour without any oscillations, as usually the occurrence of oscillation results in the loss of energy, thus keeping the efficiency of the overall solar power system optimized. This new approach not only enhances the system's performance but also yields a robust and versatile solution for real-world renewable energy systems. The proposed FLC-based MPPT algorithm is demonstrated to have significant potential for scalability and is therefore suitable for large-scale solar farms and grid systems. Its versatility and simplicity enable it to be easily integrated into demanding renewable energy setups, with guaranteed constant performance under various operating conditions. Future work will focus on designing hybrid algorithms that combine fuzzy logic with other advanced techniques, not only in the solar system but also in hybrid renewable energy systems (such as wind-solar) to further enhance tracking accuracy and computational efficiency. Additionally, the research will aim to optimize the algorithm for large-scale implementations, addressing challenges associated with grid integration and enhancing comprehensive system scalability. These efforts will pave the way for even more robust and efficient MPPT solutions in real-world solar energy applications.

List of Abbreviations and Symbols

Abbreviations			
FLC	Fuzzy Logic Controller	PV	Photovoltaic
MPPT	Maximum Power Point Tracking	CCM	Continuous Conduction Mode
MPP	Maximum Power Point	DCM	Discontinuous Conduction Mode
DC	Direct Current	NN	Neural Network
AC	Alternating Current	ΔE	Change in Error
P&O	Perturbation and Observation	S	Switch in DC/DC Converter
IC	Incremental Conductance	COA	Centroid of Area (Defuzzification Method)
PSO	Particle Swarm Optimization	BOA	Bisector of Area (Defuzzification Method)
CCM	Continuous Conduction Mode	DCM	Discontinuous Conduction Mode
GAs	Genetic Algorithms	GWO	Grey Wolf Optimization
WOA	Whale Optimization Algorithm	ACO	Ant Colony Optimization
Symbols			
I_{pv}	Photovoltaic Current Source	L	Inductance
V_{oc}	Open Circuit Voltage	C	Capacitance
I_{sc}	Short Circuit Current	V_{in}	Input Voltage
q	Electron Charge (1.602 x 10^-19 C)	V_{out}	Output Voltage
k	Boltzmann Constant (1.381 x 10^-23 J/K)	I_{Load}	Load Current
E_g	Bandgap Energy of Semiconductor	R	Resistance
ΔV_{out}	Change in Output Voltage	Z	Impedance
ΔI_{out}	Ripple Current of Load	C_1	Input Capacitor
ΔE_g	Change in Error Power	C_2	Output Capacitor
f_s	Switching Frequency	P_{pv}	Photovoltaic Power
I_D	Diode Current	β	Temperature Scaling Factor
I_{sh}	Shunt Current	DC	Direct Current
T_r	Reference Temperature (Kelvin)	AC	Alternating Current
T_c	Cell Temperature (Kelvin)	R_{sh}	Parallel Resistance
E_{g0}	Initial Bandgap Energy	D	Duty Cycle
α	Temperature Coefficient of Bandgap Energy	R_s	Series Resistance

Acknowledgement

This study was conducted at the Electrical and Automatic Research Laboratory (LREA) at the University of Yahia Fares of Medea, Algeria https://www.researchgate.net/institution/University-Yahia-Fares-of-Medea.

Author Contributions

All authors have contributed significantly, and all authors agree with the content of the manuscript.

Ethical issues

This study was approved by the Automatic Research Laboratory (EARL), University of Medea, Algeria. All participants provided written informed consent before participation.

Informed consent

Not applicable.

Funding

This work was supported by the Automatic Research Laboratory (EARL), University of Medea, Algeria. The funders had no role in study design, data collection and analysis, decision to publish, or preparation of the manuscript.

Conflict of Interest

I declare that I have no financial or personal relationships that may have inappropriately influenced me in writing this article. I confirm that this manuscript has not been published elsewhere and is not under consideration by another journal. The author declares that there are no conflicts of interest.

Data and materials availability

The data that support the findings of this study are available from Automatic Research Laboratory (EARL), University of Medea, Algeria, but restrictions apply to the availability of these data, which were used under license for the current study, and so are not publicly available. Data are however available from the authors upon reasonable request and with permission from our laboratory.

REFERENCES

1. Abdulelah AM, Ouahid B, Youcef S, Abderrezzak C, Abdelhafidh M, Ahmed M. Improve lifespan of battery energy storage in remote area power system. In: 2023 2nd International Conference on Electronics, Energy and Measurement (IC2EM). IEEE; 2023. doi: 10.1109/IC2EM59347.2023.10419419.
2. Albasheri MA, Bouchhida O, Soufı Y, Cherifi A, Mujammal MAH, Moualdia A. Energy management technique of hybrid energy storage system-based DC microgrid. J Energy Syst. 2025b;9(1):36–50. doi: 10.30521/jes.1523522
3. Albasheri MA, Bouchhida O, Soufi Y, Cherifi A, Mujammal MAH. Supervisory energy management strategy based-fuzzy logic for a DC microgrid. Int J Dyn Contr. 2025a;13(1). doi: 10.1007/s40435-024-01510-8
4. Albasheri MA, Bouchhida O, Soufi Y, Moualdia A, Mujammal M. Control and power management of DC microgrid based wind/battery/supercapacitor. In: 2022 IEEE 2nd International Maghreb Meeting of the Conference on Sciences and Techniques of Automatic Control and Computer Engineering (MI-STA). IEEE; 2022. doi: 10.1109/MI-STA54861.2022.9837665.
5. Albasheri MA, Mujammal MAH, Bouchhida O, Soufi Y, Cherifi A. Affordable clean energy through optimized hybrid microgrid design in Yemen. Research Square. 2024. doi: 10.21203/rs.3.rs-5707101/v1
6. Albasheri MA, Soufi Y, Bouchhida O, Hasan MA, Cherifi A, Khechafi S. Design, assessment and implementation of fuzzy logic for DC voltage in microgrid. In: 2025 IEEE 22nd International Multi-Conference on Systems, Signals & Devices (SSD). IEEE; 2025c; 1259–64.
7. Ali AIM, Mousa HHH, Mohamed HRA, Kamel S, Hassan AS, Alaas ZM, et al. An enhanced P&O MPPT algorithm with concise search area for grid-tied PV systems. IEEE Access. 2023;11:79408–21. doi: 10.1109/access.2023.3298106
8. Almakki ANJ. Using feedback control to control rotor flux and torque of the DFIG-based wind power system. Int J Eng Technol Innov. 2023;13(1):70–85. doi: 10.46604/ijeti.2023.10471
9. Baqir M, Channi HK. Analysis and design of solar PV system using Pvsyst software. Mater Today. 2022;48:1332–8. doi: 10.1016/j.matpr.2021.09.029
10. Basha CHH, Rani C. Different conventional and soft computing MPPT techniques for solar PV systems with high step-up boost converters: A comprehensive analysis. Energies. 2020;13(2):371. doi: 10.3390/en13020371
11. Benyoucef K, Moualdia A, Boudana D, Mujammal MAH, Albasheri MA. Optimal control strategies for DFIG-based

wind turbines: simulation and analysis. Studies Eng Exact Sci. 2024;5(3):e12580. doi: 10.54021/seesv5n3-042
12. Bhan V, Shaikh SA, Khand ZH, Ahmed T, Khan LA, Chachar FA, et al. Performance evaluation of perturb and observe algorithm for MPPT with buck–boost charge controller in photovoltaic systems. J Control Autom Electr Syst. 2021;32(6): 1652–62. doi: 10.1007/s40313-021-00781-2
13. Chuang MT, Liu YH, Ye SP. A novel variable step size incremental conductance method with an adaptive scaling factor. Appl Sci (Basel). 2020;10(15):5214. doi: 10.3390/app 10155214
14. Daradkeh YI, Tvoroshenko I. Technologies for making reliable decisions on a variety of effective factors using fuzzy logic. Int J Adv Comput Sci Appl. 2020;11(5). doi: 10.14569/ijacsa.2020 .0110507
15. Erixno O, Ramadhani F, Rahim NA, Rivai A. Realistic operation and strategic energy, economic and environmental analyses of a hybrid renewable energy based - micro combined heat and power. Sol Energy. 2024;272(112467): 112467. doi: 10.1016/j.solener.2024.112467
16. Esram T, Chapman PL. Comparison of photovoltaic array maximum power point tracking techniques. IEEE Trans Energy Convers. 2007;22(2):439–49. doi: 10.1109/tec.2006.8742 30
17. Femia A, Testa RA, Mengoni M, Rizzoli G, Vancini L, Zarri L, et al. Carrier-based PWM strategy for output current ripple minimization in multiphase motor drives. IEEE Access. 2024;12:126545–58. doi: 10.1109/access.2024.3448377
18. Gernaat DEHJ, de Boer HS, Daioglou V, Yalew SG, Müller C, van Vuuren DP. Climate change impacts on renewable energy supply. Nat Clim Chang. 2021;11(2):119–25. doi: 10.1038/s415 58-020-00949-9
19. Hoseinzadeh S, Astiaso Garcia D, Huang L. Grid-connected renewable energy systems flexibility in Norway islands' Decarbonization. Renew Sustain Energy Rev. 2023;185(1136 58):113658. doi: 10.1016/j.rser.2023.113658
20. Işen E. Modeling and Simulation of DC-DC Converters. Electronic Letters on Science and Engineering. 2021;17(1):30–41.
21. Khalid Z, Zhao L, Elahi E, Chang X. The impact of green management on green innovation in sustainable technology: moderating roles of executive environmental awareness, regulations, and ownership. Environ Dev Sustain. 2024; doi: 10.1007/s10668-024-05393-9
22. Kumar SS, Balakrishna K. A novel design and analysis of hybrid fuzzy logic MPPT controller for solar PV system under partial shading conditions. Sci Rep. 2024;14(1):10256. doi:10.10 38/s41598-024-60870-5
23. Liu F. Application of improved perturbation and observation method to photovoltaic MPPT. Proceedings of the CSU-EPSA. 2017;104.
24. Miles RW, Hynes KM, Forbes I. Photovoltaic solar cells: An overview of state-of-the-art cell development and environmental issues. Prog Cryst Growth Charact Mater. 2005;51(1–3):1–42. doi:10.1016/j.pcrysgrow.2005.10.002
25. Mohandes MA. Modeling global solar radiation using Particle Swarm Optimization (PSO). Sol Energy. 2012;86(11):3137–45. doi:10.1016/j.solener.2012.08.005
26. Mousa HHH, Youssef A-R, Mohamed EEM. Hybrid and adaptive sectors P&O MPPT algorithm based wind generation system. Renew Energy. 2020;145:1412–29. doi:10.1016/j.renene .2019.06.078
27. Mujammal M, Moualdia A, Boudana D. Improved classic direct torque control based on doubly fed induction generator use neural network. In: 2021 18th International Multi-Conference on Systems, Signals & Devices (SSD). IEEE; 2021. doi: 10.1109/SSD52085.2021.9429515.
28. Mujammal MAH, Moualdia A, Bouchhida O, Albasheri MA. Upgrade perturbation and observation of MPPT strategy via fuzzy logic controller. In: 2023 2nd International Conference on Electronics, Energy and Measurement (IC2EM). IEEE; 2023; 1–7.
29. Mujammal MAH, Moualdia A, Boudana D, Wira P, Cherifi A. Implementation of smart direct power control strategy based on M5-Pruned algorithm for three-phase pulse width modulation rectifier. Energy (Oxf). 2025;315(134417):134417. doi:10.1016/j.energy.2025.134417
30. Mujammal MAH, Moualdia A, Boulkhrachef S, Boudana D, Wira P, Albasheri MA. Next-Generation MPPT: neural network-driven optimization for superior solar performance. Studies Eng Exact Sci. 2024a;5(2):e7338. doi:10.54021/seesv5n2-150
31. Mujammal MAH, Moualdia A, Boulkhrachef S, Wira P, Boudana D, Albasheri MA. Advancing wind energy conversion: smart maximum power point based on M5-Pruned algorithm for enhanced wind energy production. Prod Eng. 2025;19(2):347–68. doi:10.1007/s11740-024-01315-w
32. Mujammal MAH, Moualdia A, Lorenzini G, Boulkhrachef S, Wira P, Albasheri MA. Three-phase PWM rectifier control: Enhanced direct power control with neural networks from theory to superior reality performance. J Eur Syst Autom. 2024;57(6):1743–52doi:10.18280/jesa.570622

33. Mujammal MAH, Moualdia A, Wira P, Albasheri MA, Cherifi A. Novel direct power control based on grid voltage modulated strategy using artificial intelligence. Smart Grids and Energy. 2024d;9(2). doi:10.1007/s40866-024-00225-1
34. Omar A-R, Haoyu W. A New High Gain DC-DC Converter With Model Predictive-Control Based MPPT Technique for Photovoltaic Systems. 2020.
35. Osheba MS, Lashine AE, Mansour AS. Design, implementation and performance evaluation of multi-function boost converter. Sci Rep. 2023;13(1):4276. doi:10.1038/s41598-023-31293-5
36. Osman MH, Ahmed MK, Refaat A, Korovkin NV. A comparative study of MPPT for PV system based on modified perturbation & observation method. In: 2021 IEEE Conference of Russian Young Researchers in Electrical and Electronic Engineering (ElConRus). IEEE; 2021.
37. Owusu-Nyarko I, Elgenedy MA, Abdelsalam I, Ahmed KH. Modified variable step-size incremental conductance MPPT technique for photovoltaic systems. Electronics (Basel). 2021;10(19):2331. doi:10.3390/electronics10192331
38. Pendem SR, Mikkili S. Modeling, simulation and performance analysis of solar PV array configurations (Series, Series–Parallel and Honey-Comb) to extract maximum power under Partial Shading Conditions. Energy Rep. 2018;4:274–87. doi:10.1016/j.egyr.2018.03.003
39. Pradhan C, Senapati MK, Ntiakoh NK, Calay RK. Roach infestation optimization MPPT algorithm for solar photovoltaic system. Electronics (Basel). 2022;11(6):927. doi:10.3390/electronics11060927
40. Premkumar M, Kumar C, Sowmya R. Mathematical modelling of solar photovoltaic cell/panel/array based on the physical parameters from the manufacturer’s datasheet. Int J Renew Energy Dev. 2020;9(1):7–22. doi:10.14710/ijred.9.1.7-22
41. Rabaia MKH, Abdelkareem MA, Sayed ET, Elsaid K, Chae K-J, Wilberforce T, et al. Environmental impacts of solar energy systems: A review. Sci Total Environ. 2021;754(141989):141989. doi: 10.1016/j.scitotenv.2020.141989
42. Ramadan A, Kamel S, El-Sehiemy RA, Khan B. Chapter 14.2 - Parameter optimization of PV modules: An overview. In: Padmanaban S, Khan B, Mahela OP, editors. Active Electrical Distribution Network. Academic Press; 2022; 401–14.
43. Salem M, Jusoh A, Dahidah M, Ishak D, Richelli A, Alhamroni I, et al. Improved topology of three-phase series resonant DC-DC boost converter with variable frequency control. Alex Eng J. 2022;61(2):1701–13. doi:10.1016/j.aej.2021.06.078
44. Salman S, Ai X, Wu Z. Design of a P-&-O algorithm based MPPT charge controller for a stand-alone 200W PV system. Prot Control Mod Power Syst. 2018;3(1). doi:10.1186/s41601-018-0099-8
45. Seeling-Hochmuth GC. A combined optimisation concet for the design and operation strategy of hybrid-PV energy systems. Sol Energy. 1997;61(2):77–87. doi:10.1016/s0038-092x(97)00028-5
46. Shaik F, Lingala SS, Veeraboina P. Effect of various parameters on the performance of solar PV power plant: a review and the experimental study. Sustainable Energy res. 2023;10(1). 10.1186/s40807-023-00076-x
47. Shang L, Guo H, Zhu W. An improved MPPT control strategy based on incremental conductance algorithm. Prot Control Mod Power Syst. 2020;5(1). doi:10.1186/s41601-020-00161-z
48. Singh S, Mathew L. Shimi SL. Design and Simulation of Intelligent Control MPPT Technique for PV Module Using MATLAB/ SIMSCAPE. Int J Adv Res Electr Electron Instrum Eng. 2013; 2(9):4554 - 4566
49. Veerachary M, Kumar N. Analysis and design of quadratic following boost converter. IEEE Trans Ind Appl. 2020;56(6):6657–73. doi:10.1109/tia.2020.3021363
50. Villegas-Mier CG, Rodriguez-Resendiz J, Álvarez-Alvarado JM, Rodriguez-Resendiz H, Herrera-Navarro AM, Rodríguez-Abreo O. Artificial Neural Networks in MPPT algorithms for optimization of photovoltaic power systems: A review. Micromachines (Basel). 2021;12(10):1260. doi: 10.3390/mi12101260
51. Wang B, Wang Q, Wei YM, Li ZP. Role of renewable energy in China’s energy security and climate change mitigation: An index decomposition analysis. Renew Sustain Energy Rev. 2018;90:187–94. doi: 10.1016/j.rser.2018.03.012